gliosis in the cerebellum is not infrequently observed in animal prion diseases. However, the cerebellar lesions observed in these guinea pigs inoculated with BSE prion have not been reported previously in animal prion diseases.

The historical classification of human prion diseases recognized the three entities of kuru, CJD and GSS; however, these diseases include a wide spectrum of histopathological phenotypes. Recent advances in protein chemistry and molecular biology have had a major influence on the classification of the clinicopathologic phenotypes of sCJD (Parchi *et al.*, 1999; Gambetti *et al.*, 2003; Cali *et al.*, 2006). According to the genotype at the polymorphic codon 129 of the PrP gene and the type of PrP^{Sc} in the brain, sCJD can be classified into six groups (MM1, MM2, MV1, MV2, VV1 and VV2; Parchi *et al.*, 1999). sCJD-VV2 is characterized by atrophy of the cerebellar cortex and matches the previously described cerebellar or ataxic variant (Cali *et al.*, 2006). In this subtype, both the molecular and the granular layers are thin and there is a severe depletion of granular cells in all areas. Although Purkinje cells are well preserved, their axons show occasional swellings and 'torpedoes' (Brownell and Oppenheimer, 1965). A diagnostic feature of this subtype is the immunolabelling pattern of the cerebellum that shows intense labelling of the Purkinje and upper granular cell layers due to the presence of numerous plaque-like formations (Gambetti *et al.*, 2003).

Kuru, the prototype human TSE, was spread by contaminated human tissues through the practice of ritual endocannibalism among the Fore people of Papua New Guinea, and the neuropathology is well established (DeArmond and Prusiner, 1997). Microscopically, the most severe pathological changes are located in the cerebellum, with the loss of granule and Purkinje cells, fusiform swelling of the proximal portion in many of the remaining Purkinje cell axons and intense radial gliosis of Bergmann astrocytes. In addition, amyloid plaques or kuru plaques are found in the granule cell layer of the cerebellar cortex, but also among Purkinje cells and in the molecular layer (DeArmond and Prusiner, 1997). Immunohistochemically, the cerebellum shows a pronounced plaque and synaptic deposition localized to the granular layer, with only infrequent molecular layer plaques (Hainfellner *et al.*, 1997; McLean *et al.*, 1998). The lesions associated with atrophy of the cerebellar cortex observed in the guinea pigs inoculated intracerebrally with BSE prions were very similar to the lesions of kuru or sCJD-VV2, although typical kuru plaques or florid plaques were not observed in the affected guinea pigs.

In contrast, the three major influences on the phenotype of the TSEs are believed to be the strain of the agent, the route of infection and the host genotype (Prusiner, 1998). Due to the oral and/or mucocutaneous route of infection, kuru is the most appropriate comparison for variant CJD (vCJD) and several articles comparing the neuropathology of these disorders have been published (Hainfellner *et al.*, 1997; Lantos *et al.*, 1997; McLean *et al.*, 1998). The neuropathological findings of these two diseases show distinct differences, particularly with respect to PrP^{CJD} immunohistochemistry; there is a much greater PrP load in all brain areas in vCJD when compared with kuru, with the exception of the cerebellar granular layer, although kuru and vCJD both have a widespread distribution of amyloid plaques (Hainfellner *et al.*, 1997; McLean *et al.*, 1998). These differences in the neuropathological profiles of kuru and vCJD cannot be explained on the basis of a common peripheral route of agent exposure, and it is suggested that the differing strains of the PrP^{CJD} agent and the genetic background could play a major role in determining the phenotype in these peripherally acquired infectious diseases (McLean *et al.*, 1998). In the transmission studies in mice (Fraser *et al.*, 1992; Bruce *et al.*, 2002), strains of scrapie and BSE have also shown the maintenance of phenotypic characteristics throughout serial passages, implying that the various isolates maintain strain-specific properties. In the transmission and serial propagation of CJD from man to guinea pigs, the inoculated animals revealed compensatory hydrocephalus as the result of marked neuronal destruction in the cerebral cortex and subcortical grey structures, with no special reference to the cerebellar lesions (Manuelidis *et al.*, 1976). Although a transmission study of sheep scrapie (Y5 strain; Horiuchi *et al.*, 2002) to guinea pigs was unsuccessful at 1,000 dpi (data not shown), a combination of the host factors with the prion strains has been thought to play a key role in influencing the disease phenotype. In addition, the pathology of the guinea pigs inoculated with the BSE prion is another very clear example of the general phenomenon that a primary TSE isolate need not produce the same phenotype following experimental transmission to that found in the natural host.

Acknowledgments

This work was supported by the Ministry of Health, Labor and Welfare of Japan (grant 20330701).

References

Brownell B, Oppenheimer DR (1965) An ataxic form of subacute presenile polioencephalopathy (Creutzfeldt–Jakob disease). *Journal of Neurology, Neurosurgery and Psychiatry*, **28**, 350–361.

Please cite this article in press as: Furuoka H et al., Predominant Involvement of the Cerebellum in Guinea Pigs Infected with Bovine Spongiform Encephalopathy (BSE), Journal of Comparative Pathology (2010), doi:10.1016/j.jcpa.2010.10.004

Bruce ME, Boyle A, Cousens S, McConnell I, Foster J *et al.* (2002) Strain characterization of natural sheep scrapie and comparison with BSE. *Journal of General Virology*, **83**, 695–704.

Cali I, Castellani R, Yuan J, Al-Shekhlee A, Cohen ML *et al.* (2006) Classification of sporadic Creutzfeldt–Jakob disease revisited. *Brain*, **129**, 2266–2277.

Cunningham C, Deacon RMJ, Chan K, Boche D, Rawlin JNP *et al.* (2005) Neuropathologically distinct prion strains give rise to similar temporal profiles of behavioral deficits. *Neurobiology of Disease*, **18**, 258–269.

DeArmond SJ, Prusiner SB (1997) Prion diseases. In: *Greenfield's Neuropathology*, 6th Edit., DI Graham, PL Lantos, Eds., Arnold, London, pp. 235–280.

DeArmond SJ, Ironside JW, Bouzamondo-Bernstein E, Peretz D (2004) Neuropathology of prion diseases. In: *Prion Biology and Diseases*, 2nd Edit., SB Prusiner, Ed., Cold Spring Harbor Laboratory Press, New York, pp. 777–856.

Debeer S, Baron T, Bencsik A (2003) Neuropathological characterization of French bovine spongiform encephalopathy cases. *Histochemistry and Cell Biology*, **120**, 513–521.

Fraser H (1979) Neuropathology of scrapie: the precision of lesions and their diversity. In: *Slow Transmissible Diseases of the Nervous System*, Vol. 1, SB Prusiner, WJ Hadlow, Eds., Academic Press, New York, pp. 387–406.

Fraser H, Bruce ME, Chree A, McConnell I, Wells GAH (1992) Transmission of bovine spongiform encephalopathy and scrapie to mice. *Journal of General Virology*, **73**, 1891–1897.

Furuoka H, Yabuzoe A, Horiuchi M, Tagawa Y, Yokoyama T *et al.* (2004) Effective antigen-retrieval method for immunohistochemical detection of abnormal isoform of prion proteins in animals. *Acta Neuropathologica*, **109**, 263–271.

Furuoka H, Yabuzoe A, Horiuchi M, Tagawa Y, Yokoyama T *et al.* (2007) Species-specificity of a panel of prion protein antibodies for the immunohistochemical study of animal and human prion diseases. *Journal of Comparative Pathology*, **136**, 9–17.

Gambetti P, Kong Q, Zou W, Parchi P, Chen SG (2003) Sporadic and familial CJD: classification and characterization. *British Medical Bulletin*, **66**, 213–239.

González L, Martin S, Begara-McGorum I, Hunter N, Houston F *et al.* (2002) Effects of agent strain and host genotype on PrP accumulation in the brain of sheep naturally and experimentally affected with scrapie. *Journal of Comparative Pathology*, **126**, 17–29.

Grassi J, Comoy E, Simon S, Creminon C, Frobert Y *et al.* (2001) Rapid test for the preclinical postmortem diagnosis of BSE in central nervous system tissue. *Veterinary Record*, **149**, 577–582.

Green R, Horrocks C, Wilkinson A, Hawkins SAJ, Ryder SJ (2005) Primary isolation of the bovine spongiform encephalopathy agent in mice: agent definition based on review of 150 transmissions. *Journal of Comparative Pathology*, **132**, 117–131.

Hainfellner JA, Liberski PP, Guiroy DC, Cervenáková L, Brown P *et al.* (1997) Pathology and immunocytochemistry of a kuru brain. *Brain Pathology*, **7**, 547–553.

Horiuchi M, Nemoto T, Ishiguro N, Furuoka H, Mohri S *et al.* (2002) Biological and biochemical characterization of sheep scrapie in Japan. *Journal of Clinical Microbiology*, **40**, 3421–3426.

Kim YS, Carp RI, Callahan SM, Wisniewski HM (1987) Incubation periods and survival times for mice injected stereotaxically with three scrapie strains in different regions. *Journal of General Virology*, **68**, 695–702.

Lantos PL, Bhatia K, Doey LJ, Al-Sarraj S, Doshi R *et al.* (1997) Is the neuropathology of new variant Creutzfeldt–Jakob disease and kuru similar? *Lancet*, **350**, 187–189.

Manuelidis L, Fritch W, Xi Y (1997) Evolution of a strain of CJD that induces BSE-like plaques. *Science*, **277**, 94–98.

Manuelidis EE, Kim J, Angelo JN, Manuelidis L (1976) Serial propagation of Creutzfeldt–Jakob disease I guinea pigs. *Proceedings of the National Academy of Sciences of the USA*, **73**, 223–227.

McLean CA, Ironside JW, Alpers MP, Brown PW, Cervenáková L *et al.* (1998) Comparative neuropathology of kuru with the variant of Creutzfeldt–Jakob disease: evidence for strain of agent predominating over genotype of host. *Brain Pathology*, **8**, 429–437.

Orge L, Simas JP, Fernandes AC, Ramos M, Galo A (2000) Similarity of the lesion profile of BSE in Portuguese cattle to that described in British cattle. *Veterinary Record*, **147**, 486–488.

Parchi P, Giese A, Capellari S, Brown P, Schulz-Schaeffer W *et al.* (1999) Classification of sporadic Creutzfeldt–Jakob disease based on molecular and phenotypic analysis of 300 subjects. *Annals of Neurology*, **46**, 224–233.

Prusiner SB (1998) Prions. *Proceedings of the National Academy of Sciences of the USA*, **95**, 13363–13383.

Spraker TR, Zink RR, Cummings BA, Wild MA, Miller MW *et al.* (2002) Comparison of histological lesions and immunohistochemical staining of proteinase-resistant prion protein in a naturally occurring spongiform encephalopathy of free-ranging mule deer (*Odocoileus hemionus*) with those of chronic wasting disease of captive mule deer. *Veterinary Pathology*, **39**, 110–119.

Wells GA, Wilesmith JW, McGill IS (1991) Bovine spongiform encephalopathy: a neuropathological prospective. *Brain Pathology*, **1**, 69–78.

Williams ES (2005) Chronic wasting disease. *Veterinary Pathology*, **42**, 530–549.

Wood JLN, McGill IS, Done SH, Bradley R (1997) Neuropathology of scrapie: a study of the distribution patterns of brain lesions in 222 cases of natural scrapie in sheep, 1982–1991. *Veterinary Record*, **140**, 167–174.

[*Received, April 14th, 2010*
Accepted, October 19th, 2010]

Please cite this article in press as: Furuoka H et al., Predominant Involvement of the Cerebellum in Guinea Pigs Infected with Bovine Spongiform Encephalopathy (BSE), Journal of Comparative Pathology (2010), doi:10.1016/j.jcpa.2010.10.004

Jpn. J. Infect. Dis., 64, 81-84, 2011

Short Communication

Atypical L-Type Bovine Spongiform Encephalopathy (L-BSE) Transmission to Cynomolgus Macaques, a Non-Human Primate

Fumiko Ono, Naomi Tase[1], Asuka Kurosawa[3], Akio Hiyaoka, Atsushi Ohyama, Yukio Tezuka, Naomi Wada[2], Yuko Sato[3], Minoru Tobiume[3], Ken'ichi Hagiwara[4], Yoshio Yamakawa[4]*, Keiji Terao[1], and Tetsutaro Sata[3]

The Corporation for Production and Research of Laboratory Primates, Tsukuba 305-0843;
[1]Tsukuba Primate Research Center, National Institute of Biomedical Innovation, Tsukuba 305-0843;
[2]Department of Veterinary Medicine, Yamaguchi University, Yamaguchi 753-8515; and
[3]Department of Pathology and [4]Department of Biochemistry and Cell Biology,
National Institute of Infectious Diseases, Tokyo 162-8640, Japan

(Received December 9, 2010. Accepted December 22, 2010)

SUMMARY: A low molecular weight type of atypical bovine spongiform encephalopathy (L-BSE) was transmitted to two cynomolgus macaques by intracerebral inoculation of a brain homogenate of cattle with atypical BSE detected in Japan. They developed neurological signs and symptoms at 19 or 20 months post-inoculation and were euthanized 6 months after the onset of total paralysis. Both the incubation period and duration of the disease were shorter than those for experimental transmission of classical BSE (C-BSE) into macaques. Although the clinical manifestations, such as tremor, myoclonic jerking, and paralysis, were similar to those induced upon C-BSE transmission, no premonitory symptoms, such as hyperekplexia and depression, were evident. Most of the abnormal prion protein (PrP^{Sc}) was confined to the tissues of the central nervous system, as determined by immunohistochemistry and Western blotting. The PrP^{Sc} glycoform that accumulated in the monkey brain showed a similar profile to that of L-BSE and consistent with that in the cattle brain used as the inoculant. PrP^{Sc} staining in the cerebral cortex showed a diffuse synaptic pattern by immunohistochemistry, whereas it accumulated as fine and coarse granules and/or small plaques in the cerebellar cortex and brain stem. Severe spongiosis spread widely in the cerebral cortex, whereas florid plaques, a hallmark of variant Creutzfeldt-Jakob disease in humans, were observed in macaques inoculated with C-BSE but not in those inoculated with L-BSE.

Bovine spongiform encephalopathy (BSE) is a fatal transmissible neurodegenerative disorder of cattle caused by the BSE prion. This disease first emerged among cattle in the United Kingdom in 1987 (1) and subsequently spread throughout Europe, Japan, and North America within the next decade (2,3). Based on similarities in disease phenotype, brain pathology, brain lesion profile, and the glycoform profile of the proteinase-resistant core of prion protein (PrP^{Sc}), it was initially believed that the disease was caused by transmission of a single prion strain conferring classical BSE (C-BSE) (4–7). However, two types of BSE, with distinct biochemical and pathological characteristics from those of C-BSE, have been detected in the European Union (EU), Japan, and the United States (8–14). These atypical BSE types have been classified as H- and L-BSE (15) in the light of the high and low molecular mass fragments of the non-glycosylated PrP molecule in the proteinase K resistant core of PrP^{Sc}. In addition, the L-type BSE prion is distinguishable by its high content of monoglycosylated molecules in the core. To date, 27 cases of L-BSE and 24 cases of H-BSE have been reported worldwide (16), thus meaning that the prevalence of atypical BSE is considerably lower than that of C-BSE. However, recent studies showed that L-BSE is easily transmissible to transgenic mice expressing human (17,18) or bovine (19,20) prion protein, as well as to non-human primates (21), with shorter incubation periods than for the transmission of C-BSE to these animals. The virulent nature of L-BSE has stimulated new concern for human public health since the transmission of C-BSE to humans resulted in variant Creutzfeldt-Jakob disease (vCJD) (4–7), a new emergent prion disease.

Since September 2001, 36 BSE cattle have been found in Japan after blanket BSE testing of approximately 10 million cattle (22) by screening and active surveillance programs conducted by the Ministry of Health, Labour and Welfare and the Ministry of Agriculture, Forestry and Fisheries (23). Two cattle, slaughtered at abattoirs, were identified as having atypical BSE by confirmatory examinations involving Western blotting (WB) and/or immunohistochemistry (IHC). Both these cases were classified as L-BSE on the basis of their glycoform profiles. The first L-BSE case was reported in a young Holstein steer (23 months old; BSE/JP8) (12), whereas the second case was reported in an old Japanese meat cow (196 months old; BSE/JP24) (13). Transmission of the first L-BSE case to bovinized mouse (transgenic

*Corresponding author: Mailing address: Department of Biochemistry and Cell Biology, National Institute of Infectious Diseases, Toyama 1-23-1, Shinjuku-ku, Tokyo 162-8640, Japan. Tel: +81-3-5285-1111 ext. 2127, Fax: +81-3-5285-1157, E-mail: yamakawa@nih.go.jp

mice over-expressing bovine PrP) was unsuccessful, probably due to the extremely low amount of PrP^{Sc} and the limited sample size (24). In contrast, the second L-BSE case was readily transmitted to both bovinized mice (25) and bovine (20,26), with shorter incubation periods than those required for the transmission of C-BSE to these animals. The glycoform profile of PrP^{Sc} propagated in the recipient animals was similar to that accumulated in the brain of the donor cattle (BSE/JP24) (20,25,26). To date, the biochemical and histopathological characteristics of the JP24 case analyzed with bovinized mice and bovine have been reported to be similar to those reported for the bovine amyloidotic spongiform encephalopathy (BASE) case, a representative L-BSE originally identified and characterized in Italy in 2003 (8,18,19). In this study, we inoculated a brain homogenate of BSE/JP24 into cynomolgus macaques to investigate disease manifestation and the characteristics of L-BSE in primates in comparison with C-BSE.

Two macaques simultaneously developed neurological signs and symptoms 19–20 months post-inoculation (mpi) with the brain homogenate of BSE/JP24. The monkeys entered the terminal stage of the disease (total paralysis) at 24–25 mpi. Both the onset and duration of the disease were shorter than those reported for the transmission of C-BSE to macaques by us and other groups (27,28). The clinical manifestations such as tremor, myoclonic jerking, and paralysis were similar to those observed during the transmission of C-BSE to macaques, whereas the premonitory abnormal behaviors, such as hyperekplexia and depression, seen upon transmission of C-BSE to macaques were not evident (27).

Histopathological analysis and IHC, performed as described previously (29), showed that severe spongiform changes and the accumulation of PrP^{Sc} with various patterns were detectable in the brains of both monkeys (Fig. 1). Vacuolization was profound throughout the cerebral cortex, from the frontal to the occipital lobes (Fig. 1a). Likewise, synaptic-type PrP^{Sc} precipitation (30) was observed in the whole cerebral cortex and basal ganglia by IHC (Figs. 1b and c). Dense precipitates and plaques of PrP^{Sc}, which had been observed in cattle (JP24) brain (13), were not detected in the cerebrum of the monkeys. PrP^{Sc}, in the form of small plaques or coarse granules, was, however, detected in the molecular layer of the cerebellum (Fig. 1e). Despite the severe spongiosis in the cerebral cortex, florid plaques, which are large PrP^{Sc} plaques surrounded by vacuoles, a hallmark of vCJD (4–7,30) and C-BSE transmission to macaques (27,28), were not observed. The histopathology of the brain was therefore similar to that reported for the brain of L-BSE (BASE)-transmitted macaques (21).

Figure 2 shows the results of WB analysis of PrP^{Sc} in the brain and peripheral nerves (dorsal root ganglia). Despite the region-specific morphology of PrP^{Sc} deposition, the proportions of the di/mono/non-glycosylated forms of PrP^{Sc} propagated in various regions of the

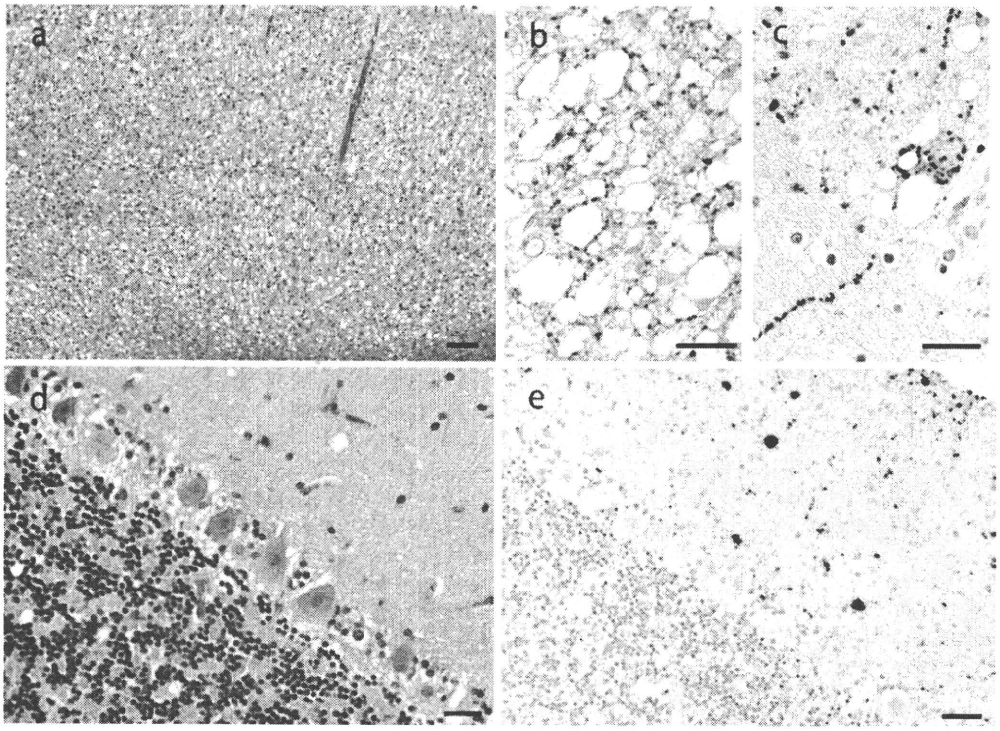

Fig. 1. Histopathology (HE) and PrP^{Sc} immunostaining of monkey brain. HE-staining of brain sections corresponding to the cortex of the cerebrum (a) and the cerebellum (d); PrP^{Sc} immunostaining of the cerebral cortex (b) and basal ganglia (c) and the cerebellum (e); a consecutive section of (d). Bar = 100 μm (a); 20 mm (b, c, d, and e). HE- and PrP^{Sc} immunostaining were performed as described previously (29). Anti-prion protein antibody T4, a rabbit polyclonal antibody raised against the synthetic peptide correspond to codons 211–239 of bovine prion protein (38), was used as the primary antibody. The CSA II amplification system (Biotin-free Catalyzed Amplification System; Dako, Kyoto, Japan) was used to enhance signal intensity instead of the Envision + immuno-enhancing system.

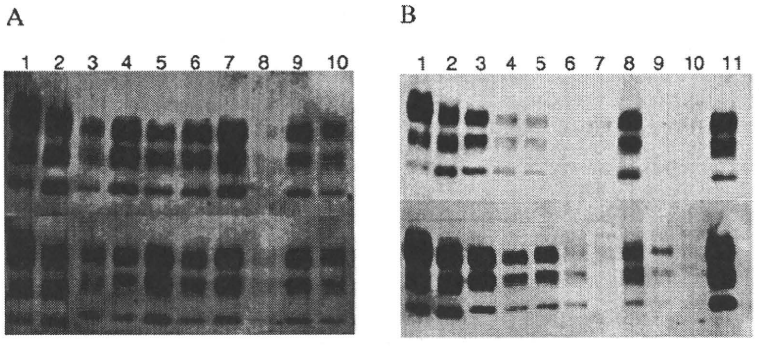

Fig. 2. PrP^{Sc} accumulated in the brain (A) and peripheral nerves (B) of euthanized monkeys. Upper and lower panels represent the brains of different monkeys, #14 and #15, respectively. (A) Lane 1, PrP^{Sc} of C-BSE (25 μg tissue equivalent); lane 2, PrP^{Sc} of L-BSE (50 μg equivalent); lanes 3–10, PrP^{Sc} accumulated in the brain of a monkey (10 μg brain tissue equivalent): lane 3, frontal lobe; lane 4, temporal lobe; lane 5, parietal lobe; lane 6, occipital lobe; lane 7, thalamus; lane 8, mid brain/medula oblongata; lane 9, cerebellum; lane 10, olfactory bulb. (B) Lanes 1–2, PrP^{Sc} of C-, L-BSE (25 and 50 μg brain equivalent); lanes 3–6, spinal cord of cervical thoracic and lumber regions (200 μg tissue equivalent): lane 6, dorsal root ganglia (1 mg tissue equivalent); lane 7, optic nerve (1 mg tissue equivalent); lane 8, retina (1 mg tissue equivalent); lane 9, trigeminal nerve (1 mg tissue equivalent); lane 10, sciatic nerve (5 mg tissue equivalent); lane 11, olfactory bulb (20 μg tissue equivalent). All techniques used in this analysis, including preparation of tissue homogenates, proteinase K treatment, poly-acrylamide gel electrophoresis on 12% gels (NuPAGE; Invitrogen, Carlsbad, Calif., USA) and transfer of protein onto PVDF membrane, were performed as described previously (27,29). Anti-prion protein antibody 6H4 (mouse monoclonal; Roche Applied Science, Basel, Switzerland) and peroxidase-labeled anti-mouse IgG antibody $(Fab)_2$, were used as the primary and secondary antibodies, respectively. Immunoreactive protein on the blot was reacted with ECLplus chemiluminescent reagent and signals were recorded and processed on a Lumino-image analyzer LAS-3000 mini (Fuji film, Tokyo, Japan). PrP^{Sc} of C-BSE and L-BSE were prepared from cattle brain by the same method and electrophoresed as in-house references to evaluate the whole process.

brain were similar to each other and to those observed in the original JP24 cattle (Fig. 2A). Although it appeared that the non-glycosylated PrP^{Sc} accumulated in the monkey tissue showed a slight upper-shift of its electrophoretic mobility towards that of C-BSE in the present WB analysis (for example, Fig. 2A lower panel), it is not known whether this minor shift was significant as the non-glycosylated PrP^{Sc} in the BSE/JP24 cattle originally had a mobility similar to, or only slightly different from, that of the C-BSE case (13,25). Further transmission experiments and a more accurate WB analysis are therefore needed to confirm such subtle differences in the non-glycosylated molecule of BSE prions after transmission to macaques. Both IHC and WB successfully detected PrP^{Sc} in retina, trigeminal ganglia, and dorsal root ganglia (Fig. 2B). PrP^{Sc} was barely detected in the sciatic nerve of monkey #15 by WB (Fig. 2B lowere panel lane 10). However, the amount of PrP^{Sc} in the sciatic nerve was estimated to be less than 1/1,000 of the cerebral PrP^{Sc}. Deposition of PrP^{Sc} in lymphoid tissues (spleen and tonsils) or lymph nodes (inguinal, axillary, submandibular, deep cervical, mesenteric, subiliac, and hilar lymph nodes) was not detected by IHC or WB. Considering the sensitivity of WB analysis and the amount of tissue (5 mg/lane) used in this experiment, the amount of PrP^{Sc} in lymphoid tissues must therefore be lower than 1/5,000 of that in the brain.

The results of an enzyme-linked immunosorbent assay for bovine PrP^{Sc} (BSE TeSeE; BioRad, Mornes-la-Coquette, France) suggested that the amount of PrP^{Sc} in the inoculum used in this study was as low as 1/5 than in a brain homogenate of C-BSE (JP6; $10^{5.2}$ LD_{50}/g using bovinized mice; see ref. 24) previously used for the transmission of C-BSE to macaques (27). Despite the low concentration of PrP^{Sc}, both the incubation period and the duration of the disease were approximately 2/3 shorter than those required for the transmission of C-BSE to macaques, although they were similar to those reported for the transmission of BASE to macaques (21). These results may therefore indicate that the L-BSE agent is more virulent in non-human primates. However, further experiments involving oral administration would be required to assess the risk of L-BSE transmission from affected cattle to humans through the consumption of beef products.

We were unable to detect PrP^{Sc} in lymphatic tissues or lymph nodes by WB or IHC. However, this does not necessarily indicate the absence of infectivity of those organs. Determination of the infectivity using inbred mice was difficult since they are reportedly insensitive or have limited sensitivity, if any, to L-BSE (25,31). The BSE/JP24 isolate could not be transmitted to three different lines of inbred mice, even 700 days after inoculation (Hagiwara, unpublished). Further analysis using transgenic mice expressing bovine or human PrP, or in vitro amplification of PrP^{Sc} by protein misfolding cyclic amplification (32,33) or quaking-induced conversion (34), would be necessary to detect trace amounts of PrP^{Sc} or infectivity in the lymphatic tissues or lymph nodes of the macaques.

The origin of atypical BSE is generally unknown, except for one H-BSE case in the United States that is considered to result from a heritable pathogenic mutation in the PrP gene (35). Epidemiological evidence (8–10,13,15) suggests that most cases of atypical BSE are found in old cattle (>8 years of age), and the relatively even birth-year distributions lead to speculation that atypical BSE is a sporadic prion disorder of cattle similar to sporadic CJD in humans (36). In this context, the conversion of BASE prion and other L-BSE prions

into C-BSE-like phenotypes during interspecies transmission to inbred mice or transgenic mice expressing ovine PrP has been reported (31,37,38). These findings are therefore of interest as regards the origin of BSE and the possible divergent evolution of prion strains.

Acknowledgments This work was supported by a grant for BSE research from the Ministry of Health, Labour and Welfare, Japan (H20-Shokuhin-Ippan-008).

Conflict of interest None to declare.

REFERENCES

1. Wells, G.A.H., Scott, A.C., Johnson, C.T., et. al. (1987): A novel progressive spongiform encephalopathy in cattle. Vet. Rec., 121, 419-420.
2. World Organization for Animal Health. Numbers of Cases of Bovine Spongiform Encephalopathy (BSE) Report in the United Kingdom. Online at 〈http://www.oie.int/eng/info/en_esbru_original.htm〉.
3. World Organization for Animal Health. Numbers of Cases of Bovine Spongiform Encephalopathy (BSE) in Farm Cattle Worldwide (excluding the United Kingdom). Online at 〈http://www.oie.int/eng/info/copie2_en_esbmonde.htm〉.
4. Will, R.G., Ironside, J.W., Zeidler, M., et al.(1996): A new variant of Creutzfeldt-Jakob disease in the UK. Lancet, 347, 921-925.
5. Collinge, J., Sidle, K.C.L., Meads, J., et al. (1996): Molecular analysis of prion strain variation and the aetiology of 'new variant' CJD. Nature, 383, 685-690.
6. Hill, A.F., Desbruslais, M., Joiner, S., et al. (1997): The same prion strain causes vCJD and BSE. Nature, 389, 448-450.
7. Bruce, M.E., Will, R.G., Ironside, J.W., et al. (1997): Transmission to mice indicate that 'new variant' CJD is caused by the BSE agent. Nature, 389, 498-501.
8. Casalone, C., Zanusso, G., Acutis, P., et al (2004): Identification of a second bovine amyloidotic spongiform encephalopathy: molecular similarities with sporadic Creutzfeldt-Jakob disease. Proc. Natl. Acad. Sci. USA, 101, 3065-3070.
9. Biacabe, A-G., Laplanche, J-L., Ryder, S., et al. (2004): Distinct molecular phenotypes in bovine prion diseases. EMBO Rep., 5, 110-115.
10. Bushmann, A., Gretzschel, A., Biacabe, A.-G., et al. (2006): Atypical BSE in Germany-proof of transmissibility and biochemical characterization. Vet. Microbiol., 117, 103-116.
11. Baron, T.G.M., Biacabe, A-G., Bencsik, A., et al. (2006): Transmission of new bovine prion to mice. Emg. Infect. Dis., 12, 1125-1128.
12. Yamakawa, Y., Hagiwara, K., Nohtomi, K., et al. (2003): Atypical proteinase K-resistant prion protein (PrP^{res}) observed in an apparently healthy 23-month-old Holstein steer. Jpn. J. Infect. Dis., 56, 221-222.
13. Hagiwara, K., Yamakawa, Y., Sato, Y., et al. (2007): Accumulation of mono-glycosylated form-rich, plaque-forming PrP^{Sc} in the second atypical bovine spongiform encephalopathy case in Japan. Jpn. J. Infect. Dis., 60, 305-308.
14. Richt, J.A., Kunkle, R.A., Nicholson, E.M., et al. (2007): Identification of two bovine spongiform encephalopathy cases diagnosed in the United States. J. Vet. Diagn. Invest., 19, 142-154.
15. Jacobs, J.G., Langeveld, J-P.M., Biacabe, A-G., et al. (2007): Molecular discrimination of atypical bovine spongiform encephalopathy strain from geographical region spanning a wide area in Europe. J. Clin. Microbiol., 45, 1821-1829.
16. Stack, M.J., Focosi-Snyman, R., Cawthraw, S., et al. (2009): Third atypical BSE case in Great Britain with an H-type molecular profile. Vet. Rec., 14, 605-606.
17. Béringue, V., Herzog, L., Reine, F., et al. (2008): Transmission of atypical bovine prion to mice transgenic for human prion protein. Emerg. Infect. Dis., 14, 1898-1901.
18. Kong, Q., Zheng, M., Casalone, C., et al. (2008): Evaluation of the human transmission risk of an atypical bovine spongiform encephalopathy prion strain. J. Virol., 82, 3697-3701.
19. Lombardi, G., Casalone, C., D'Angelo, A., et al. (2008): Interspecies transmission of BASE induces clinical dullness and amyotrophic change. PLoS Pathog., 4, e1000075.
20. Fukuda, S., Iwamura, Y., Imamura, M., et al. (2009): Interspecies transmission of L-type-like bovine spongiform encephalopathy detected in Japan. Microbiol. Immunol., 53, 704-707.
21. Comoy, E.E., Casalone, C., Lescoutra-Etchegaray, N., et al. (2008): Atypical BSE (BASE) transmitted from asymptomatic aging cattle to a primate. PLoS ONE, 3, e3017.
22. Ministry of Health, Labour and Welfare: Results on the BSE Screening. Online at 〈http://www.mhlw.go.jp/houdou/0110/h1018-6.html〉 (in Japanese).
23. Yamanouchi, K. and Yoshikawa, Y. (2007): Bovine spongiform encephalopathy (BSE) safety measure in Japan. J. Vet. Med. Sci., 69, 1-6.
24. Yokoyama, T., Masujin, K., Yamakawa, Y., et al. (2007): Experimental transmission of two young and one suspended bovine spongiform encephalopathy (BSE) cases to bovinized transgenic mice. Jpn. J. Infect. Dis., 60, 317-320.
25. Masujin, K., Shu, Y., Yamakawa, Y., et al. (2008): Biological and biochemical characterization of L-type-like bovine spongiform encephalopathy (BSE) in Japanese black cattle. Prion, 2, 123-128.
26. Iwamaru, Y., Imamura, M., Matsuura, Y., et al. (2009): Accumulation of L-type bovine prions in peripheral nerve tissues. Emeg. Infect. Dis., 16, 1151-1154.
27. Ono, F., Terao, K., Tase, N., et al. (2011): Experimental transmission of bovine spongiform encephalopathy (BSE) to cynomolgus macaques, a non-human primate. Jpn. J. Infect. Dis., 64, 50-54.
28. Lasmézas, C.I., Deslys, J-P., Demaimay, R., et al. (1996): BSE transmission to macaques. Nature, 381, 743-744.
29. Iwata, N., Sato, Y., Higuchi, Y., et al. (2006): Distribution of PrP^{Sc} in cattle with bovine spongiform encephalopathy slaughtered at abattoirs in Japan. Jpn. J. Infect. Dis. 59, 100-107.
30. Liberski, P.P and Ironside, J.W. (2005): Neuropathology of transmissible spongiform encephalopathies (prion diseases). p. 13-48. *In* Brown, D.R. (ed.), Neurodegeneration and Prion Diseases. Springer, New York.
31. Capobianco, R., Casalone, C., Suardi, S., et al. (2007): Conversion of the BASE prion strain into the BSE strain: the origin of BSE? PLoS Pathog., 3, e31.
32. Saborio, G.P., Permanne, P. and Soto, C. (2001): Sensitive detection of prion protein by cyclic amplification of protein misfolding. Nature, 411, 810-813.
33. Chen, B., Morales, R., Barria, M.A., et al. (2010): Estimating prion concentration in fluids and tissue by quantitative PMCA. Nat. Methods, 7, 519-520.
34. Atarashi, R., Wilham, J.M., Christensen, L., et al. (2010): Simplified ultrasensitive prion detection by recombinant PrP conversion with shaking. Nat. Methods, 5, 211-212.
35. Richt, J.A. and Hall, S.M. (2008): BSE case associated with prion protein gene mutation. PLoS Pathog., 4, e1000156.
36. Brown, P., McShane, L.M., Zanusso, G., et al. (2006): On the question of sporadic or atypical bovine spongiform encephalopathy and Creutzfeldt-Jakob diseases. Emerg. Infect. Dis., 12, 1816-1821.
37. Béringue, V., Andréoletti, O., Le Dur, A., et al. (2007): A bovine prion acquires an epidemic bovine spongiform encephalopathy strain-like phenotype on interspecies transmission. J. Neurosci., 27, 6965-6971.
38. Takahashi, H., Takahashi, R.H., Hasegawa, H., et al. (1999): Characterization of antibodies raised against bovine PrP-peptides. J. Neurovirol., 5, 300-307.

Jpn. J. Infect. Dis., 64, 50-54, 2011

Original Article

Experimental Transmission of Bovine Spongiform Encephalopathy (BSE) to Cynomolgus Macaques, a Non-Human Primate

Fumiko Ono, Keiji Terao[1], Naomi Tase[1], Akio Hiyaoka, Atsushi Ohyama, Yukio Tezuka, Naomi Wada[2], Asuka Kurosawa[3], Yuko Sato[3], Minoru Tobiume[3], Ken'ichi Hagiwara[4], Yoshio Yamakawa[4]*, and Tetsutaro Sata[3]

The Corporation for Production and Research of Laboratory Primate, Tsukuba 305-0843;
[1]Tsukuba Primate Research Center, National Institute of Biomedical Innovation, Tsukuba 305-0843;
[2]Department of Veterinary Medicine, Yamaguchi University, Yamaguchi 357-8515; and
[3]Department of Pathology and [4]Department of Biochemistry and Cell Biology,
National Institute of Infectious Diseases, Tokyo 162-8640, Japan

(Received December 9, 2010. Accepted December 22, 2010)

SUMMARY: Bovine spongiform encephalopathy (BSE) was transmitted to three macaques by intracerebral inoculation of a brain homogenate from affected cattle detected in Japan. All monkeys developed abnormal behavioral signs, such as intermittent anorexia and hyperekplexia, around 24 months after inoculation. Neuronal symptoms, such as tremor, myoclonic jerking, and paralysis, appeared 27–44 months after inoculation. These symptoms worsened and total paralysis ensued within a year after onset. The disease duration was approximately 8–12 months. Both the incubation period and the duration of disease were shortened in the secondary transmission experiment to macaques. Heavy accumulation of disease-causing conformer(s) of prion protein (PrP^{Sc}), with a similar glycoform profile to the PrP^{Sc} contained in the inoculum, and severe spongiform changes in the histology of the brain, confirmed the successful transmission of BSE to monkeys. Florid plaques, a characteristic histological hallmark of variant Creutzfeldt-Jakob disease, were prominent in the cerebral cortex, in which a prion antigen was detected by immunohistochemistry (IHC). PrP^{Sc} was mostly confined to the central nervous system, although small amounts of PrP^{Sc} accumulated in the peripheral nerves of monkeys, as detected by Western blotting (WB). Neither IHC nor WB detected PrP^{Sc} in the lymphatic organs/tissues, such as the tonsils, spleen, and appendix.

INTRODUCTION

Transmissible spongiform encephalopathies, or prion diseases, are fatal neurodegenerative disorders characterized by severe spongiform changes and the accumulation of abnormal form(s) of prion protein (PrP^{Sc}) in the central nervous system (CNS) (1-3). PrP^{Sc} is a disease-causing conformer(s) of PrP encoded on the host DNA (4,5) that exhibits, with a few exceptions, partial resistance to digestion by proteinase K (1). Human prion diseases are known to be either sporadic, genetic or infectious disorders, such as sporadic Creutzfeldt-Jakob disease (CJD), Gerstmann-Straüssler-Scheinker syndrome, fatal familial insomnia, or kuru, iatrogenic CJD, and variant CJD (vCJD), respectively (1,6). In ruminants, the diseases emerge as scrapie in sheep and goats (1), bovine spongiform encephalopathy (BSE) in cattle (1,7), and chronic wasting disease in elk and deer (1).

vCJD was first recognized in 1996 as a CJD-like fatal neurological disorder that emerged among teenagers in the UK (6). The brain pathology and biochemical characteristics associated with PrP^{Sc} strongly suggested that vCJD was induced by the causative agent of BSE upon the consumption of meat products contaminated by risk materials such as the CNS and/or spinal ganglia of BSE-affected cattle (8–10). As a result of the BSE pandemic, more than 223 CJD patients have been identified to date across the world, with 175 cases in the UK and 48 cases in 10 other countries (11). The annual incidence of vCJD has been reported to be in decline, although some reports predict that the number of vCJD patients may reach some 136,000 in the future, depending on the incubation period of BSE in humans (12–14).

The emergence of vCJD raised another public-health concern regarding the possible iatrogenic transmission of the disease from human to human through blood transfusion or the administration of biological products of human origin, because of the peripheral distribution of PrP^{Sc} in lymphoid follicles of the tonsils and appendix (15,16) even before the onset of clinical symptoms (17). To date, at least three definite cases of transfusion-associated vCJD infection have been reported (11). Appropriate animal models for vCJD are therefore greatly needed in order to study the pathogenesis of the disease and to develop therapeutic interventions.

In this study, we report the pathological and biochemical analyses of an animal model for vCJD using cynomolgus macaques inoculated with classical-type BSE prion isolated from Japanese cattle. We also report a second successful transmission experiment.

*Corresponding author: Mailing address: Department of Biochemistry and Cell Biology, National Institute of Infectious Diseases, Toyama 1-23-1, Shinjuku-ku, Tokyo 162-8640, Japan. Tel: +81-3-5285-1111 ext. 2127, Fax: +81-3-5285-1157, E-mail: yamakawa@nih.go.jp

MATERIALS AND METHODS

Monkeys: The cynomolgus macaques used in this experiment were bred at the Tsukuba Primate Research Center at the National Institutes of Biomedical Innovation (Ibaraki, Japan). All monkeys were male and were 2–2.4 years old when inoculated. The amino acids at codons 129 and 219 of the prion protein gene (Prnp) were methionine/methionine (M/M) and glutamic acid/glutamic acid (E/E), respectively. Monkeys were bred and dissected in biosafety level 3 facilities according to the Biosafety Guidelines of the National Institute of Biomedical Innovation and the National Institute of Infectious Diseases (Tokyo, Japan). The Animal Ethics Committee and the Animal Care and Use Committee at the National Institute of Biomedical Innovation approved this study.

Inoculum: The inoculum was prepared from the brain tissue of BSE cattle (classical-BSE [C-BSE], BSE/JP6) which had been detected in 2003 as a result of the BSE inspection program (18). A 10% homogenate (w/v) of the brain was prepared by shaking the brain tissue (thalamic region) with zirconia beads (d = 2 mm; Nikkato, Tokyo, Japan) in PBS for 5 min using a Multi-beads Shocker apparatus (Yasui Kikai, Tokyo, Japan). This homogenate was then stored at −80°C until use. Prior to inoculation, the homogenate was further dispersed by brief sonication. Two hundred microliters of the homogenate was introduced into the hypothalamus on the right side of the brain using 23G needles, which were passed through a hole in the skull made by a micro-drill. The position of the distal end of the needle was adjusted using brain map coordination under anesthesia with ketamine-HCl and xylazine. A brain homogenate of a diseased monkey (#7) was also prepared as an inoculum for the second transmission.

Histopathology and immunohistochemistry (IHC): For histological examination and IHC, tissue samples were fixed in buffered formalin, treated with formic acid, and processed as described previously (19). The sections were prepared and subjected to routine histological examination by hematoxylin and eosin (HE) staining and IHC. For the IHC of PrP^{Sc}, the sections were pretreated by hydrolytic autoclaving in 1 mM HCl at 121°C for 20 min or 100 mM NaOH, 2% NaCl and 0.1% *N*-lauroylsarcosine at 60°C for 10 min (20). Endogenous peroxidase activity was blocked with 0.3% hydrogen peroxide in 100% methanol for 30 min at room temperature. The sections were treated with an anti-prion protein antibody T4, a rabbit polyclonal antibody (21). The Envision$^+$ system (Dako, Kyoto, Japan) was used for signal detection. A negative control section derived from a healthy monkey was also subjected to IHC.

Preparation of PrP^{Sc} and Western blotting (WB): Tissue homogenates (5–20% (w/v) depending on the sample size) were prepared by shaking diced tissues with zirconia beads (d = 2 mm) in PBS as described above. PrP^{Sc} was prepared by successive hydrolysis of homogenates with DNase, collagenase, and proteinase K in 50 mM Tris-HCl buffer pH 7.5 containing 0.1 M NaCl and 2% twittergent 4-12, and precipitated by the addition of a 0.5 volume of 2-butanol/methanol mixture (5:1, v/v) containing 3 mM phenylmethylsulfonyl fluoride, as described previously (19). The precipitate was dissolved in a minimum volume (10–40 μl) of SDS-sample buffer (0.065 M Tris-HCl buffer pH 6.8 containing 5% glycerol, 3 mM ethylenediaminetetraacetic acid, 5% sodium dodecyl sulfate, 4% β-mercaptoethanol, and 0.04% bromophenol blue) and heated for 5 min at 100°C. The sample, with or without dilution, was electrophoresed in a 12% NuPAGE polyacrylamide gel with NuPAGE MOPS SDS running buffer (Invitrogen, Carlsbad, Calif., USA), then the proteins were electrophoretically transferred onto PVDF membrane in a NuPAGE transfer buffer (Invitrogen) following the manufacturer's instructions. The membrane was blocked by soaking in 50 mM Tris-HCl buffer, pH 7.5, containing 10% non-fat milk and 5% fetal calf serum. The blot was then incubated with anti-prion protein monoclonal antibody 6H4 (Prionics AG, Zurich, Switzerland) (0.125 μg/ml) followed by a horseradish peroxidase-conjugated sheep antibody $(Fab')_2$ against mouse IgG (NA 9310; Amersham Biosciences, Piscataway, N.J., USA). An ECLplus detection kit (Amersham Biosciences) was used to detect immunoreactive proteins and the signal was recorded and processed using an image analyzer (LAS-3000-mini; Fuji Film, Tokyo Japan). The detection threshold for PrP^{Sc} by WB was estimated to be equivalent to 1 μg of brain tissue (data not shown).

RESULTS

Clinical signs and symptoms: The clinical signs and symptoms observed during the course of the disease are listed in Table 1. Upon primary inoculation, two of the three monkeys (#7 and #10) simultaneously developed abnormal behavioral signs, such as intermittent anorexia and hyperekplexia, 26 and 27 months post-inoculation (mpi). Neurological disorders, such as tremor, myoclonic jerking, and paralysis, became apparent at 29 and 27 mpi. All monkeys displayed total paralysis at the terminal stage of the disease (35–37 mpi). The third monkey (#11) also developed similar symptoms,

Table 1. Signs and symptoms observed during the transmission of BSE to macaques

Transmission	Primary			Secondary	
Monkey #	#7	#10	#11	#16	#17
Inoculated age (mo)	24	28	29	25	24
Onset (mo)	29	27	44	15	13
Disease duration (mo)	8	8	15	5	6
Abnormal behaviors:					
Depression	−	+++	−	+	−
Self harm behavior	+	−	+	−	−
Anorexia	+	−	+	−	+
Scordinema	−	+	−	−	−
Hyperekplexia	+++	+++	++	++	++
Neuronal symptoms:					
Ataxia	+++	+++	+++	++	+++
Tumor	+++	+++	+++	+	++
Myoclonus	++	++	++	−	++
Paralysis	+++	++	+++	+	++
Astasia	+++	++	+++	−	+

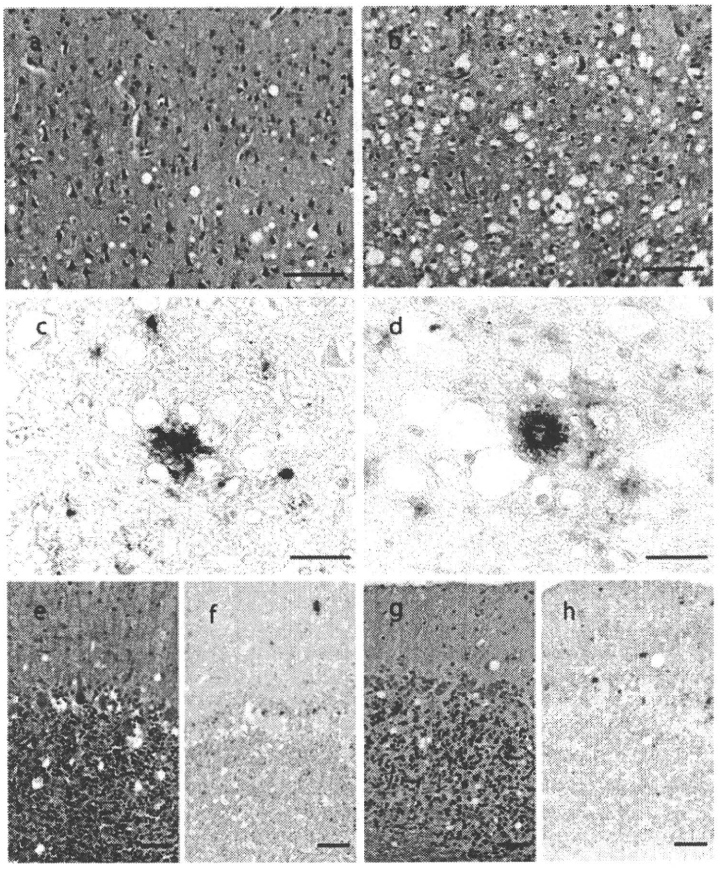

Fig. 1. Histology and immunohistochemistry (IHC) of PrP^{Sc} in the brains of macaques transmitted with BSE. Parts a, b, e, and g represent HE staining of the cerebral (a, b) or cerebellar (e, g) cortex of primary transmitted (a, e) or secondary BSE transmitted monkeys, respectively. Parts c, d, f, and h represent IHC of PrP^{Sc} in the cerebral (c, d) and cerebellar (f, h) cortex of primary (c, f) or secondary (d, h) BSE transmitted monkeys. Bar = 100 μm (a, b, e, f, g, and h); 50 μm (c and d).

although onset of the disease was delayed to 45 mpi, which is around 1.5 years longer than for the other monkeys.

In the secondary transmission experiment, a brain homogenate of a euthanized monkey (#7) was prepared and inoculated into two monkeys. They developed symptoms similar to those observed during the first (interspecies) transmission experiment, although the incubation period and duration of the disease were markedly shortened to 16 months and 6 months, respectively, thereby indicating adaptation of the prion to monkeys.

Histopathological analysis and IHC of the CNS of monkeys: The results of histopathological analysis and IHC of the monkey brains are shown in Fig. 1. Severe spongiform changes and the accumulation of PrP^{Sc} in the brain were detected in all monkeys. Vacuolization was more marked at the cortex of the frontal and temporal lobes (Figs. 1a and b) than in the occipital lobe and cerebellum (data not shown). Florid plaques, a dense core of PrP^{Sc} surrounded by vacuoles, were located at the cerebral cortex (Figs. 1c and d). The deposition of PrP^{Sc} with form of small plaques or coarse granules or fine glanules was found in the molecular or granular layer of the cerebellum, respectively (Figs. 1f and h), whereas fine granular deposits of PrP^{Sc} were observed in the brain of BSE cattle (19). Granular deposition of PrP^{Sc} was also found in the gray matter of the spinal cord, with mild spongiform changes. A small but consistent accumulation of PrP^{Sc} was found in the ganglionic cell layer, inner plexiform layer, and outer plexiform layer of the retina, and in the ganglionic and satellite cells of the trigeminal and dorsal root ganglia without vacuolation (data not shown).

Both spongiform changes (Figs. 1a and b) and the numbers of florid plaques of PrP^{Sc} became severe in the brains of the secondary transmission experiment.

WB and distribution of PrP^{Sc}: The WB results for PrP^{Sc} propagated in monkey brain are shown in Fig. 2a. The glycoform profiles of PrP^{Sc} propagated in each monkey brain are apparently indistinguishable from each other and are likely identical to that of PrP^{Sc} accumulated in the cattle brain. The glycoform profiles of PrP^{Sc} prepared from various brain regions and the spinal cord of monkey #7 were also identical, as shown in Fig. 2b. To explore the occurrence of PrP^{Sc} outside the CNS, homogenates of peripheral nerves (vagus, median, intercostal, sympathetic, sciatic and celiac plexus), lymphatic tissues (spleen, tonsil, and distal ileum), and lymph nodes (inguinal, axillary, submandibular, deep cervices, mesenteric, subiliac, and hilar) were prepared and analyzed by WB. PrP^{Sc} was detected in several peripheral nerves and the submandibular lymph node of

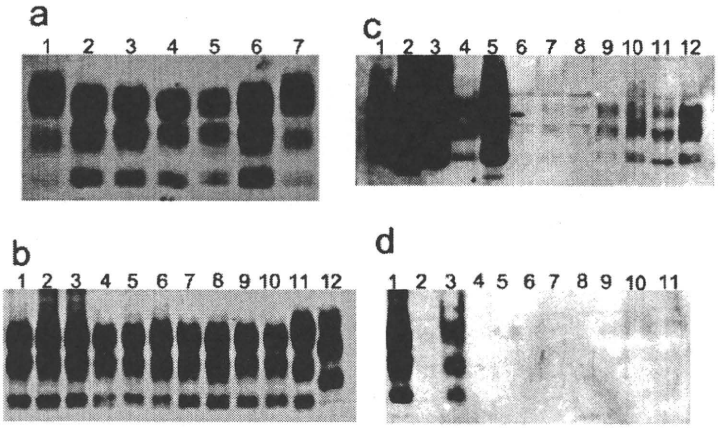

Fig. 2. Distribution of PrP^{Sc}, as analyzed by Western blotting. (a) Western blot of PrP^{Sc} of bovine and macaques. Lanes 1 and 7 represent bovine PrP^{Sc} (100 μg tissue equivalent) of C-BSE; lanes 2–6 represent PrP^{Sc} propagated in monkey brain (12.5 μg tissue equivalent). Samples were prepared from the thalamic region of primary transmitted monkeys: #7 (lane 2), #10 (lane 3), and #11 (lane 4), or secondary transmitted monkeys: #16 (lane 5) and #17 (lane 6). (b) PrP^{Sc} propagated in the CNS of monkey #7 (primary transmission). Lane 1, frontal lobe (8.3); lane 2, parietal lobe (8.3); lane 3, temporal lobe (8.3); lane 4, occipital lobe (19.6); lane 5, thalamus (33.2); lane 6, cerebellum; lane 7, midbrain (14.6); lane 8, pons (22.2); lane 9, medulla oblongata (44.4); lane 10, spinal cord (208); lane 11, bovine PrP^{Sc} (50); lane 12, human PrP^{Sc} (CJD type 1 [40]). Figures in parentheses represent the amounts of tissue equivalents (μg) applied to the well. (c) PrP^{Sc} propagated in the peripheral nerves of monkey #7 (primary transmission). Lane 1, PrP^{Sc} in brain (positive control 0.015); lane 2, olfactory bulb (0.5); lane 3, optic nerve (5); lane 4, retina (0.5); lane 5, trigeminal nerve (0.5); lane 6, celiac ganglia (5); lanes 7 and 8, vagus nerves (5); lane 9, median nerve (5); lane 10, intercostal nerve (5); lane 11, sympathetic nerve (5); lane 12, sciatic nerve (5). Figures in parentheses represent the amounts of tissue equivalents (mg) applied to the well. (d) Extra-neuronal PrP^{Sc} of monkey #7 (primary transmission). Lane 1, brain (positive control 0.008); lane 2, mesenteric lymph node (7.5); lane 3, submandibular lymph node (7.5); lane 4, axillary lymph node (7.5); lane 5, inguinal lymph node (7.5); lane 6, hilar lymph node (7.5); lane 7, thymus (7.5); lane 8, distal ileum (7.5); lane 9, tonsil (7.5); lane 10, spleen (7.5); lane 11, adrenal grand (7.5). Figures in parentheses represent the amounts of tissue equivalents (mg) applied to the well.

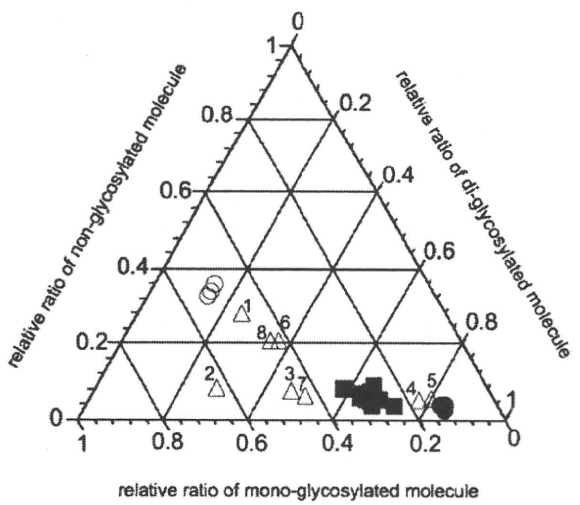

Fig. 3. Comparison of the glycoform profiles of PrP^{Sc} propagated in monkey #7. ○, sporadic CJD MM1; ●, BSE; ■, PrP^{Sc} in brain and spinal cord; △: PrP^{Sc} in 1, sympathetic nerve; 2, trigeminal nerve; 3, sciatic nerve; 4, optic nerve; 5, retina; 6, submandibular lymph node; 7, median nerve; 8, vagus nerve.

monkey #7, as demonstrated in Figs. 2c and d. The sciatic nerve of monkey #10 was also positive for PrP^{Sc}. Interestingly, the peripheral PrP^{Sc} had an apparently different glycoform profile from that of PrP^{Sc} purified from the CNS, as shown in Fig. 3. The amount of PrP^{Sc} in the peripheral nerves and lymphatic tissues/lymph nodes of other monkeys were below the detection limit of WB analysis. Considering the sensitivity of WB analysis (as low as 1 μg brain tissue, see Materials and Methods) and the amount of tissue (5 mg/lane) used in this experiment, the amount of PrP^{Sc} in the peripheral nerves is likely to be lower than 1/1,000 of that in brain tissue.

DISCUSSION

A non-human primate model has been shown to be a suitable model for humans and has often been applied to preclinical trials of compounds or biologicals for potential human use. With regard to a human vCJD model, as described herein, non-human primates are invaluable because they have been shown to develop florid plaques in the brain, as observed in vCJD patients, and the molecular signature of the prion by WB analysis is similar to those of vCJD patients and BSE-affected cattle. Such pathological features are difficult to reproduce in inbred mice.

We successfully performed experimental transmission of BSE to cynomolgus macaques by the intracerebral inoculation of brain homogenates of asymptomatic BSE cattle detected in Japan. The clinical symptoms, brain pathology, and characteristics of PrP^{Sc} observed in this study were essentially the same as those obtained in earlier European BSE transmission experiments in macaques (22,23). These results strongly indicate that the BSE prion used in the present study, an isolate from the BSE/JP6 cow, is of the same strain as the BSE prion prevailing in European countries, thereby supporting the notion that the agent spread from Europe to Japan.

PrP^{Sc} has frequently been detected in the lymphoid follicles of lymphatic tissues, such as the tonsils and appendix of vCJD patients and orally transmitted BSE monkeys (24–26), whereas in this study we were unable to detect PrP^{Sc} in these organs even when tissues were collected from monkeys at a terminal stage of the illness. Most of the lymph nodes (inguinal, axillary, submandibular, deep cervical, mesenteric, subiliac, and hilar) were also negative for PrP^{Sc}, and we were barely able to detect PrP^{Sc} in the submandibular lymph nodes of monkey #7 by WB. These findings indicate the presence of small amounts of PrP^{Sc} in other lymph nodes and possibly in lymphatic tissues and organs. However, the amounts of PrP^{Sc} in lymphatic tissues or lymph nodes might be dependent on the invasion route of the infective agent. We are currently performing parallel experiments in which we directly introduced 1 ml of 10% brain homogenates two times with a week interval into the stomach of three monkeys using a catheter. Even though the amount of inoculum used in this oral-challenge experiment is 10 times higher than that used for the intercerebral transmission experiment, to date none of the monkeys have developed abnormal neuronal signs 7.5 years post-inoculation.

PrP^{Sc} was uniformly detected in retina, trigeminal ganglia, and dorsal root ganglia of monkeys by both IHC and WB. The amount of PrP^{Sc} in peripheral nerves decreased dramatically, with the exception of the CNS, probably due to centrifugal distribution from the brain.

The glycoform profiles of PrP^{Sc} propagated in the CNS of monkeys were almost identical, and were similar, if not identical, to the PrP^{Sc} glycoforms in cattle brain, although with higher ratios of monoglycosylated molecules being present in the PrP^{Sc} of monkeys compared with the PrP^{Sc} in cattle brain. In addition, the diversity of glycoform profiles among PrP^{Sc} propagated in the peripheral nerves and lymph nodes of monkey #7 was evident (Fig. 3). Further characterization of this peripheral PrP^{Sc} was difficult due to the limited amounts of samples available, although it is worth noting that alterations occur in the biochemical characteristics of BSE prions during interspecies transmission (27–30).

Acknowledgments This work was supported by a grant for BSE research from the Ministry of Health, Labour and Welfare, Japan (H20-Shokuhin-Ippan-008).

Conflict of interest None to declare.

REFERENCES

1. Prusiner, S.B. (2004): An introduction to prion biology and diseases. p. 1–87. *In* S. B. Prusiner (ed.), Prion Biology and Diseases. 2nd ed. (ISBN 0-87969-693-1). Cold Spring Harbor Laboratory Press, Cold Spring Harbor.
2. Prusiner, S.B. (1982): Novel proteinaceous infectious particles cause scrapie. Science, 216, 136–144.
3. Prusiner, S.B. (1991): Molecular Biology of Prion Diseases. Science, 252, 1515–1522.
4. Chesebro, B., Race, R., Wehrly, K., et al. (1985): Identification of scrapie prion-specific mRNA in scrapie-infected and uninfected brain. Nature, 315, 331–333.
5. Oesch, B., Westaway, D., Wälchli, M., et al. (1985): A cellular gene encodes scrapie PrP 27-30 protein. Cell, 40, 735–746.
6. Will, R.G., Ironside, J.W., Zeidler, M., et al. (1996): A new variant of Creutzfeldt-Jakob disease in the UK. Lancet, 347, 921–925.
7. Wells, G.A.H., Scott, A.C., Johnson, C.T., et al. (1987): A novel progressive spongiform encephalopathy in cattle. Vet. Rec., 121, 419–420.
8. Collinge, J., Sidle, K.C.L., Meads, J., et al. (1996): Molecular analysis of prion strain variation and the aetiology of 'new variant' CJD. Nature, 383, 685–690.
9. Hill, A.F., Desbruslais. M., Joiner, S., et al. (1997): The same prion strain causes vCJD and BSE. Nature, 389, 448–450.
10. Bruce, M.E., Will, R.G., Ironside, J.W., et al. (1997): Transmission to mice indicate that 'new variant' CJD is caused by the BSE agent. Nature, 389, 498–501.
11. The National Creutzfeldt-Jakob Disease Surveillance Unit (NCJDSU), The University of Edinburgh. Variant Creutzfeldt-Jakob Disease Current Data (OCTOBER 2010). Online at 〈http://www.cjd.ed.ac.uk/vcjdworld.htm〉.
12. Ghani, A.C., Ferfuson, N.M., Donnelly, C.A. et al. (2000): Predicted vCJD mortality in Great Britain. Nature, 406, 583–584.
13. Valleron, A.-J., Boelle, P.-Y., Will, R., et al. (2001): Estimation of epidemic size and incubation time based on age characteristics of vCJD in the United Kingdom. Science, 294, 1726–1728.
14. Clarke, P. and Ghani, A.C., (2005): Projections of the future course of the primary vCJD in the UK: inclusion of subclincal infection and the possibility of wider genetic susceptibility. J. R. Soc. Interface, 2, 19–31.
15. Hilton, D.A., Ghani, A.C., Conyers, L., et al. (2002): Accumulation of prion protein in tonsil and appendix: review of tissue samples. Br. Med. J., 325, 633–634.
16. Hill, A.F., Butterworth, R.J., Joiner, S., et al. (1999): Investigation of variant Creutzfeldt-Jakob disease and other human prion diseases with tonsil biopsy samples. Lancet, 353, 183–189.
17. Hilton, D.A., Fathers, E., Edwards, P., et al. (1998): Prion immunoreactivity in appendix before onset of variant Creutzfeldt-Jakob disease. Lancet, 352, 703–704.
18. Yamanouchi, K. and Yoshikawa, Y. (2007): Bovine spongiform encephalopathy (BSE) safety measures in Japan. J. Vet. Med. Sci., 69, 1–6.
19. Iwata, N., Sato, Y., Higuchi, Y., et al. (2006): Distribution of PrP^{Sc} in cattle with bovine spongiform encephalopathy slaughtered at abattoirs in Japan. Jpn. J. Infect. Dis., 59, 100–107.
20. Bencsik, A.A., Debeer, S.O.S. and Baron, T.G.M. (2005): An alternative pretreatment procedure in animal transmissible spongiform encephalopathies diagnosis using PrPsc immunohistochemistry. J. Histochem. Cytochem., 53, 1199–1202.
21. Takahashi, H., Takahashi, R., Hasegawa, H., et al. (1999): Characterization of antibodies raised against bovine PrP-peptides. J. Neurovirol., 5, 300–307.
22. Lasmézas, C.I., Deslys, J.-P., Demaimay. R., et al. (1996): BSE transmission to macaques. Nature, 381, 743–744.
23. Lasmézas, C.I, Fournier, J.-G., Nouvel, V., et al. (2001): Adaptation of the bovine spongiform encephalopathy agent to primates and comparison with Creutzfeldt-Jakob disease: implications for human health. Proc. Natl. Acad. Sci. USA, 98, 4142–4147.
24. Herzog, C., Salès. N., Etchegaray, N., et al. (2004): Tissue distribution of bovine spongiform encephalopathy agent in primates after intravenous or oral infection. Lancet, 363, 422–428.
25. Herzog, C., Rivière, J., Lescoutra-Etchegaray, N., et al. (2005): PrP^{TSE} distribution in a primate model of variant, sporadic, and iatrogenic Creutzfeldt-Jakob disease. J. Virol., 79, 14339–14345.
26. Lasmézas, C.I., Comoy, E., Hawkins, S., et al. (2005): Risk of oral infection with bovine spongiform encephalopathy agent in primates. Lancet, 365, 781–783.
27. Asante, E.A., Linehan, J.M., Desbruslais, M., et al. (2002): BSE prions propagate as either variant CJD-like or sporadic CJD-like prion strains in transgenic mice expressing human prion protein. EMBO J., 21, 6358–6366.
28. Capobianco, R., Casalone, C., Suardi, S., et al. (2007): Conversion of the BASE prion strain into the BSE strain: the origin of BSE? PLoS Pathog., 3, e31 (doi:10.1371/journal.ppat.0030031).
29. Béringue, V., Andréoletti, O., Le Dur, A., et al. (2007): A bovine prion acquires an epidemic bovine spongiform encephalopathy strain-like phenotype on interspecies transmission. J. Neurosci., 27, 6965–6971.
30. Yokoyama, T., Masujin, K., Iwamaru, Y., et al. (2009): Alteration of the biological and biochemical characteristics of bovine spongiform encephalopathy prions during interspecies transmission in transgenic mice model. J. Gen. Virol., 90, 261–268.

Biochemical and Biophysical Research Communications 397 (2010) 505–508

Contents lists available at ScienceDirect

Biochemical and Biophysical Research Communications

journal homepage: www.elsevier.com/locate/ybbrc

An improved method for cell-to-cell transmission of infectious prion

Masahiko Tanaka [a,b], Hideyuki Hara [a], Hiroshi Nishina [b], Kentaro Hanada [a], Ken'ichi Hagiwara [a,*], Tomohiko Maehama [a,**]

[a] Department of Biochemistry and Cell Biology, National Institute of Infectious Diseases, 1-23-1 Toyama, Shinjuku-ku, Tokyo 162-8640, Japan
[b] Developmental and Regenerative Biology, Tokyo Medical and Dental University, 1-5-45 Yushima, Bunkyo-ku, Tokyo 113-8510, Japan

ARTICLE INFO

Article history:
Received 24 May 2010
Available online 31 May 2010

Keywords:
Prion
Transmission
Co-culture method

ABSTRACT

Prion diseases are characterized by the accumulation of a pathological form of prion protein (PrP^{Sc}), which behaves as an infectious agent. Here we developed an *in vitro* co-culture system to analyze the PrP^{Sc} transmission from ScN2a cell, which persistently retains PrP^{Sc}, to naïve N2a cell. In this cell-to-cell transmission system, PrP^{Sc} transmitted to recipient N2a cell was able to be detected within 5–7 days. Further characterization showed that higher cell density greatly facilitated the transmission of PrP^{Sc}. This improved *in vitro* transmission method may become a useful tool for unveiling the molecular mechanism of PrP^{Sc} transmission.

1. Introduction

Prion diseases are neurodegenerative disorders associated with the accumulation of a protease-resistant form of prion protein (PrP). A number of studies have suggested that the protease-resistant isoform of PrP is generated as a result of conformational change of PrP [1,2]. The protease-resistant PrP, which is also designated as PrP^{Sc} when indicating a disease-causing infectious agent, is known to transmit from "infected" cell to naïve cell [3]. PrP is anchored to the cell surface by glycosylphosphatidylinositol moiety; thus proteins that participate in PrP maturation process and surface expression process may affect both PrP^{Sc} transmission and propagation. However, certain cellular factors involved in the transmission process still remain largely unknown.

In order to unveil the mechanism underlying this cell-to-cell transmission process, several *in vitro* transmission models, based on co-culture strategy, have been established [4–8]. However, these co-culture protocols require several weeks to detect transmitted PrP^{Sc}; therefore an improvement in the *in vitro* PrP^{Sc} transmission system would greatly contribute to the understanding of its molecular mechanism. In this study, we developed a novel *in vitro* transmission method using ScN2a cell (as a PrP^{Sc} donor) and N2a cell (as a recipient) and demonstrated that co-culture of these cells allowed us to detect transmitted PrP^{Sc} within 5–7 days.

* Corresponding author. Fax: +81 3 5285 1157.
** Corresponding author. Fax: +81 3 5285 1157.
E-mail addresses: hagiwark@nih.go.jp (K. Hagiwara), tmaehama@nih.go.jp (T. Maehama).

0006-291X/$ - see front matter © 2010 Elsevier Inc. All rights reserved.
doi:10.1016/j.bbrc.2010.05.143

2. Materials and methods

2.1. Cell culture

Mouse N2a cells and ScN2a cells were maintained as described previously [3,9]. N2a-MHM2 cells [10] were cultured as same as above cell lines, except the addition of G418 to 500 μg/ml.

Co-culture for the PrP^{Res} transmission was conducted as follow. First, ScN2a cells were treated with 10 μg/ml of mitomycin C (MC) for 2 h, then 4×10^5 N2a and 4×10^5 MC-treated ScN2a cells were mixed and plated onto a 6-cm dish. After the incubation for 4 days at 37 °C with 5% CO_2, the cells were trypsinized, diluted at 1:5, and plated onto a new vessel. The cells were further cultured for 3 days, then cell lysates were prepared to analyze PrP as described below.

2.2. Immunoblot analysis

All following procedures were conducted at 4 °C unless specified. Cells grown on a 6-cm dish were rinsed with phosphate-buffered saline then dissolved in 1 ml of Lysis buffer consisting of 20 mM Tris–HCl (pH 7.6), 100 mM NaCl, 0.5% (w/v) Triton X-100, and 0.2% (w/v) sodium deoxycholate. After removal of insoluble materials by centrifugation (1500g, 5 min), each lysate was diluted to 1 mg of protein/ml with Lysis buffer, then 10 μg of proteinase K (PK) was added to 800 μl of the lysate. Protein concentration was determined using BradfordUltra Kit (Expedeon Protein Solutions) and bovine serum albumin as a standard protein. After 1-h incubation at 37 °C, 20 μl of 0.1 M phenylmethylsulfonyl fluoride was added to terminate the PK reaction. PK-resistant protein aggregates were then collected with 10 μg of blue dextran by

centrifugation (90,700g, 1 h). Precipitates were washed with 500 μl of 0.01 M phenylmethylsulfonyl fluoride (in methanol) and dissolved into 40 μl of modified Laemmli buffer (62.5 mM Tris–HCl (pH 6.8), 13 mM sodium ethylenediaminetetraacetate, 2 M urea, 5% (v/v) glycerol, 4% (v/v) β-mercaptoethanol, 5% (w/v) sodium dodecyl sulfate, and 0.04% (w/v) bromophenol blue). Proteins were resolved on SDS–polyacrylamide gel and transferred to polyvinylidene fluoride membrane filter. Cell lysate (10 μg of protein) which was not treated by PK was also used in order to analyze total amount of PrP. The filter was probed with specified antibodies as described previously [9,11]. Primary antibodies used are anti-PrP 6H4 (Prionics, 1:5000) and anti-PrP 3F4 (Millipore, 1:5000). Typical images from repeated experiments are represented in each figure.

3. Results and discussion

In order to establish an *in vitro* cell-to-cell PrP^{Sc} transmission system with high efficiency, we chose ScN2a cell, which has been widely used as persistent PrP^{Sc}-infected cell, as a PrP^{Sc} donor cell and parental N2a cell as a recipient cell. We first treated ScN2a cells with mitomycin C (MC), a potent inhibitor of DNA synthesis, at 10 μg/ml for 2 h, which completely inhibited the donor cell proliferation (data not shown). MC-treated ScN2a cells and naïve N2a cells were trypsinized and each of 4×10^5 cells was plated onto a 6-cm dish. As shown in Fig. 1A, PrP^{Sc} was observed in cells after 3-day co-culture. For control experiment, either 4×10^5 of N2a cells or MC-treated ScN2a cells were individually cultured, then cell lysates were prepared and merged when collected. It is of note that comparable amount of PrP^{Sc} was also observed in the lysate of control "separated" culture (Fig. 1B), suggesting that most of this PK-resistant PrP observed at day 3 was self-propagated PrP^{Sc} in donor cells. Therefore, to dilute out the PrP^{Sc} propagated in donor cells, the cells were trypsinized and replated onto a new dish with 1:5 dilution at day 4. After the trypsinization/dilution, PrP^{Sc} was no longer observed in control (separately cultured) cells (Fig. 1B). In contrast, PrP^{Sc} was observed even at day 5 in co-cultured cell lysate, and the level of PrP^{Sc} was increased during the culture (Fig. 1A). These observations suggest that PrP^{Sc} developed in the co-culture might be originally transmitted from donor cells and propagated in recipient N2a cells. However, there remains the possibility that ScN2a cells restarted proliferation under the co-culture condition even after MC treatment, and PrP^{Sc} was propagated in growing ScN2a cells. In order to exclude this possibility, we next used N2a-MHM2 cell as a recipient cell instead of N2a cell. N2a-MHM2 cell stably expresses PrP-MHM2, a mouse/hamster chimera PrP encompassing Met-Lys-His-Met (hamster) epitope instead of Leu-Lys-His-Val (mouse) at amino acid residues 108–111 (Fig. 2A). PrP-MHM2 is able to be distinguished from mouse PrP by using anti-PrP 3F4 antibody which selectively recognizes the Met-Lys-His-Met epitope [10]. N2a-MHM2 cells were cultured with ScN2a cells under exactly same condition as described in above ScN2a/N2a co-culture scheme, then existence of "PK-resistant" PrP-MHM2 in cell lysate was tested using the 3F4 antibody. As shown in Fig. 2B and C, "PK-resistant" PrP-MHM2 definitely appeared in the cell lysate of N2a-MHM2 cells which had been cultured with ScN2a cells for 7 days. It should be noted that endogenous PrP^{Sc} propagated in ScN2a cells never be recognized by 3F4 antibody due to its epitope selectivity (Fig. 2B). These results, taken together, clearly demonstrated that the conversion of PrP-MHM2 from PK-sensitive form to PK-resistant form in the recipient cells (*i.e.*, N2a-MHM2 cells) occurred in the presence of PrP^{Sc} provided by the donor cells (*i.e.*, ScN2a cells). In addition, the immunoblot analysis using 6H4 antibody (Fig. 2C) shows that the total amount of PrP in N2a-MHM2 cells was larger than that in N2a cells; however development of "PK-resistant" PrP (both PrP-MHM2 and endogenous mouse PrP) in N2a-MHM2 cells by the co-culture with ScN2a cells was less efficient when compared to that in N2a cells. This result indicates that N2a cell acts as a superior recipient for PrP^{Sc} in our assay system. Therefore, we used this cell line for further analyses.

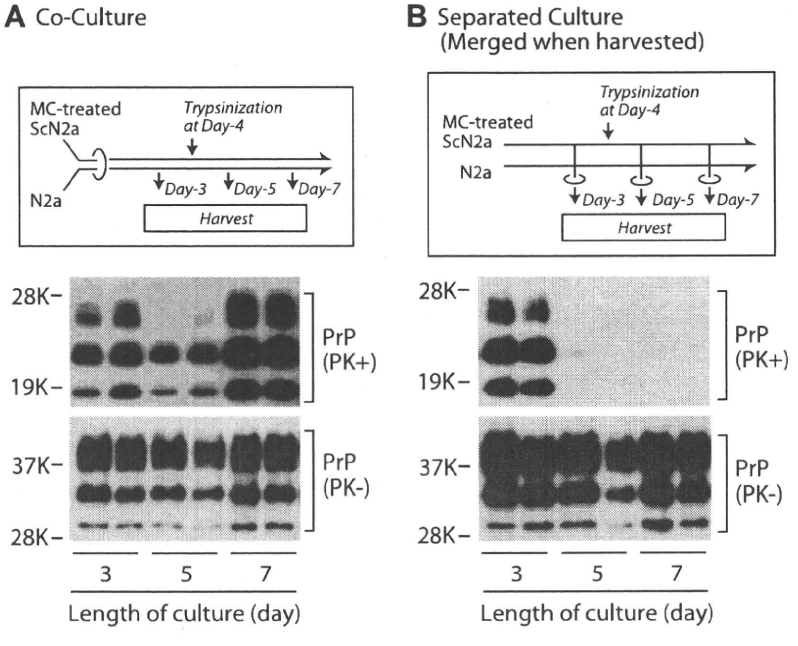

Fig. 1. PrP^{Sc} was propagated in N2a cells when co-cultured with ScN2a cells. (A) N2a cells (4×10^5) were cultured with MC-treated ScN2a cells (4×10^5) as described in "Section 2." At day-3, -5, and -7, cell lysates were prepared, and PrP (lower panel) and PK-resistant PrP (upper panel) were analyzed using anti-PrP 6H4 antibody. (B) N2a cells (4×10^5) and MC-treated ScN2a cells (4×10^5) were independently cultured for indicated length with trypsinization/replating step at day-4. When harvested, cell lysates from these cultures were merged and PrP (lower panel) and PK-resistant PrP (upper panel) were analyzed as described above. The positions of molecular-weight markers are indicated in each panel.

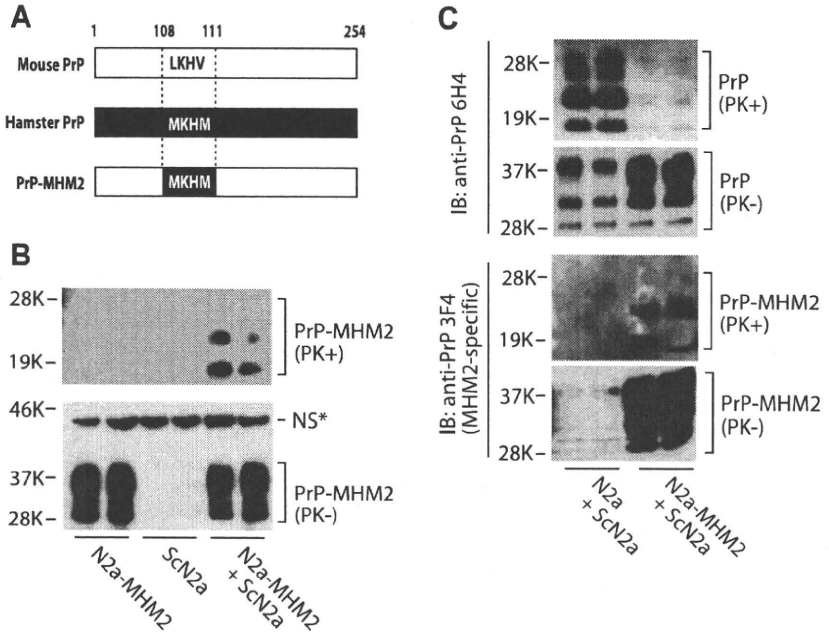

Fig. 2. PrP^{Sc} was transmitted from ScN2a cell to naïve recipient cell. (A) Mouse/Hamster chimera PrP-MHM2. PrP-MHM2 has "MKHM" motif (108–111), the epitope for anti-PrP 3F4 antibody. (B) N2a-MHM2 cells (4×10^5) and MC-treated ScN2a cells (4×10^5) were co-cultured or independently cultured for 7 days with trypsinization/replating step at day-4, then PrP-MHM2 (lower panel) and PK-resistant PrP-MHM2 (upper panel) were analyzed using anti-PrP 3F4 antibody. Note that non-specific band (*NS*) confirms equal loading of samples. (C) Either N2a cells or N2a-MHM2 cells were co-cultured with MC-treated ScN2a cells for 7 days as described above. PrP species were analyzed using anti-PrP 6H4 antibody or anti-PrP 3F4 antibody as shown in the figure. The positions of molecular-weight markers are indicated in each panel.

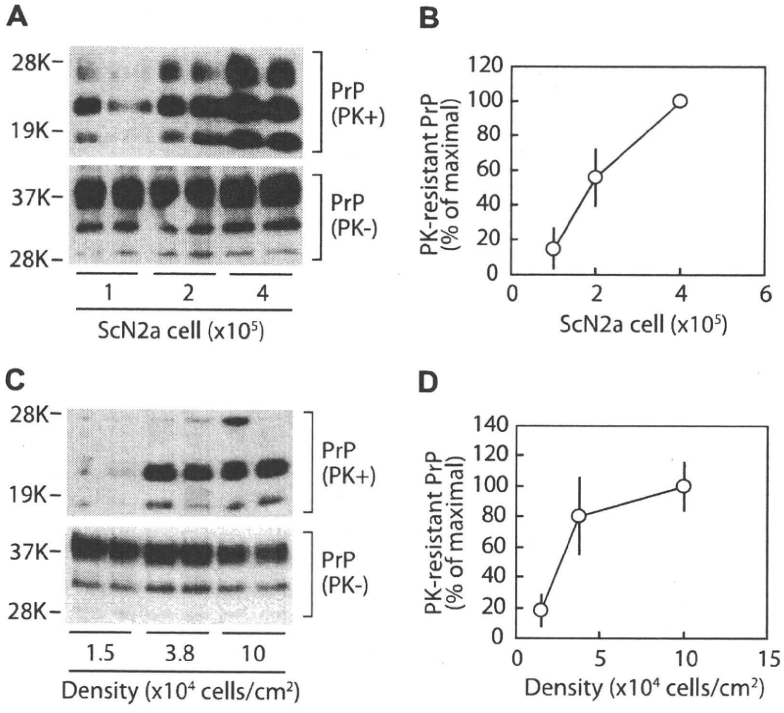

Fig. 3. Transmission of PrP^{Sc} was affected by cell density. (A) N2a cells (4×10^5) were cultured with indicated number of MC-treated ScN2a cells. After 7-day culture, PrP (lower panel) and PK-resistant PrP (upper panel) were analyzed using anti-PrP 6H4 antibody. (B) The relative intensity of non-glycosylated form of PK-resistant PrP was measured by the ImageJ program and plotted as average ± range from duplicated experiment. (C) N2a cells (4×10^5) were cultured with MC-treated ScN2a cells (4×10^5) on either 10-cm (1.5×10^4 cells/cm^2), 6-cm (3.8×10^4 cells/cm^2), or 3.5-cm (1.0×10^5 cells/cm^2) dish. After 7-day culture, PrP (lower panel) and PK-resistant PrP (upper panel) were analyzed using anti-PrP 6H4 antibody. (D) Non-glycosylated form of PK-resistant PrP was quantitated as described above. The positions of molecular-weight markers are indicated in each panel.

Next we asked how many donor cells were required for efficient transmission of PrP^{Sc}. As shown in Fig. 3A and B, when initial number of donor cell was decreased, PrP^{Sc} population developed in the recipient N2a cells was substantially decreased. This result let us ask whether PrP^{Sc} transmission was affected by the number of donor cell or cell density. In addition, recent report demonstrated that cell density largely affected PrP^{Sc} propagation in ScN2a cells [12]. Therefore, we next carried out the co-culture with fixed number of donor and recipient cells in three different culture vessels in order to test the effect of cell density on PrP^{Sc} transmission. When the co-culture was performed at 1.5×10^4 cells/cm^2, development of PrP^{Sc} was almost abolished (Fig. 3C and D). In contrast, with the cell density of more than 3.8×10^4 cells/cm^2, with which the culture reached to confluent at day 1, almost similar amount of PrP^{Sc} was developed during 7-day culture. These results suggest the requirement of cell-to-cell contact for the transmission and propagation of PrP^{Sc} *in vitro*.

In this study, we successfully established a novel PrP^{Sc} transmission model with which the transmission was detectable within 5–7 days. Spreading of PrP^{Sc} both *in vitro* and *in vivo* may have two steps; intercellular transmission and intracellular propagation. Recent study showed that the inhibition of ceramide synthesis resulted in increased propagation of PrP^{Sc} in ScN2a cells [13]. Surprisingly, in our co-culture model, we noticed that administration of fumonisin B1, a ceramide synthase inhibitor, to the culture decreased PrP^{Sc} accumulation in the recipient N2a cells (unpublished observations), while we also observed that fumonisin B1 treatment increased PrP^{Sc} accumulation in ScN2a cells in agreement with previous report [12]. These observations imply that intercellular transmission and intracellular propagation employ distinct mechanisms, in which certain molecules may provide opposite effect on PrP^{Sc} development in the cell. Our model may become useful to distinguish each step of PrP^{Sc} spreading. In addition, our model would have great advantage in testing the effect of exogenous gene expression and/or gene knockdown on the PrP^{Sc} transmission, because 5- to 7-day culture to detect the PrP^{Sc} transmission allows us to use conventional transient transfection techniques. It is now under investigation to identify cellular factors that participate in the PrP^{Sc} transmission process using knockdown screening strategy with our PrP^{Sc} transmission model.

Acknowledgments

This work was supported by Grants-in-Aid for Scientific Research (19370058, 20054024 and 21657035) from the Japanese Ministry of Education, Culture, Sports, Science and Technology and Grants-in-Aid for BSE Research (20330701) from the Japanese Ministry of Health, Labour and Welfare.

References

[1] R.K. Meyer, M.P. McKinley, K.A. Bowman, M.B. Braunfeld, R.A. Barry, S.B. Prusiner, Separation and properties of cellular and scrapie prion proteins, Proc. Natl. Acad. Sci. USA 83 (1986) 2310–2314.
[2] S.B. Prusiner, M.R. Scott, S.J. DeArmond, F.E. Cohen, Prion protein biology, Cell 93 (1998) 337–348.
[3] D.A. Butler, M.R. Scott, J.M. Bockman, D.R. Borchelt, A. Taraboulos, K.K. Hsiao, D.T. Kingsbury, S.B. Prusiner, Scrapie-infected murine neuroblastoma cells produce protease-resistant prion proteins, J. Virol. 62 (1988) 1558–1564.
[4] S. Alais, S. Simoes, D. Baas, S. Lehmann, G. Raposo, J.L. Darlix, P. Leblanc, Mouse neuroblastoma cells release prion infectivity associated with exosomal vesicles, Biol. Cell 100 (2008) 603–615.
[5] S. Ghaemmaghami, P.W. Phuan, B. Perkins, J. Ullman, B.C. May, F.E. Cohen, S.B. Prusiner, Cell division modulates prion accumulation in cultured cells, Proc. Natl. Acad. Sci. USA 104 (2007) 17971–17976.
[6] N. Kanu, Y. Imokawa, D.N. Drechsel, R.A. Williamson, C.R. Birkett, C.J. Bostock, J.P. Brockes, Transfer of scrapie prion infectivity by cell contact in culture, Curr. Biol. 12 (2002) 523–530.
[7] N. Nishida, S. Katamine, L. Manuelidis, Reciprocal interference between specific CJD and scrapie agents in neural cell cultures, Science 310 (2005) 493–496.
[8] S. Paquet, C. Langevin, J. Chapuis, G.S. Jackson, H. Laude, D. Vilette, Efficient dissemination of prions through preferential transmission to nearby cells, J. Gen. Virol. 88 (2007) 706–713.
[9] Y. Okemoto-Nakamura, Y. Yamakawa, K. Hanada, K. Tanaka, M. Miura, I. Tanida, M. Nishijima, K. Hagiwara, Synthetic fibril peptide promotes clearance of scrapie prion protein by lysosomal degradation, Microbiol. Immunol. 52 (2008) 357–365.
[10] M.R. Scott, R. Kohler, D. Foster, S.B. Prusiner, Chimeric prion protein expression in cultured cells and transgenic mice, Protein Sci. 1 (1992) 986–997.
[11] T. Maehama, M. Tanaka, H. Nishina, M. Murakami, Y. Kanaho, K. Hanada, RalA functions as an indispensable signal mediator for the nutrient-sensing system, J. Biol. Chem. 283 (2008) 35053–35059.
[12] S. Nakamitsu, A. Kurokawa, T. Yamasaki, M. Uryu, R. Hasebe, M. Horiuchi, Cell density-dependent increase in the level of protease-resistant prion protein in prion-infected Neuro2a mouse neuroblastoma cells, J. Gen. Virol. 91 (2010) 563–569.
[13] N. Naslavsky, H. Shmeeda, G. Friedlander, A. Yanai, A.H. Futerman, Y. Barenholz, A. Taraboulos, Sphingolipid depletion increases formation of the scrapie prion protein in neuroblastoma cells infected with prions, J. Biol. Chem. 274 (1999) 20763–20771.

Shinkai-Ouchi *et al. Proteome Science* 2010, **8**:53
http://www.proteomesci.com/content/8/1/53

PROTEOME SCIENCE

RESEARCH Open Access

Identification and structural analysis of C-terminally truncated collapsin response mediator protein-2 in a murine model of prion diseases

Fumiko Shinkai-Ouchi[1], Yoshio Yamakawa[1], Hideyuki Hara[1], Minoru Tobiume[2], Masahiro Nishijima[1,3], Kentaro Hanada[1], Ken'ichi Hagiwara[1*]

Abstract

Background: Prion diseases are fatal neurodegenerative disorders that accompany an accumulation of the disease-associated form(s) of prion protein (PrP^{Sc}) in the central nervous system. The neuropathological changes in the brain begin with focal deposits of PrP^{Sc}, followed by pathomorphological abnormalities of axon terminal degeneration, synaptic loss, atrophy of dendritic trees, and eventual neuronal cell death in the lesions. However, the underlying molecular basis for these neuropathogenic abnormalities is not fully understood.

Results: In a proteomic analysis of soluble proteins in the brains of mice challenged intracerebrally with scrapie prion (Obihiro I strain), we found that the amount of the full-length form of collapsin response mediator protein-2 (CRMP-2; 61 kDa) decreased in the late stages of the disease, while the amount of its truncated form (56 kDa) increased to comparable levels observed for the full-length form. Detailed analysis by liquid chromatography-electrospray ionization-tandem mass spectrometry showed that the 56-kDa form (named CRMP-2-ΔC) lacked the sequence from $serine^{518}$ to the C-terminus, including the C-terminal phosphorylation sites important for the regulation of axonal growth and axon-dendrite specification in developing neurons. The invariable size of the mRNA transcript in Northern blot analysis suggested that the truncation was due to post-translational proteolysis. By overexpression of CRMP-2-ΔC in primary cultured neurons, we observed the augmentation of the development of neurite branch tips to the same levels as for $CRMP\text{-}2^{T514A/T555A}$, a non-phosphorylated mimic of the full-length protein. This suggests that the increased level of CRMP-2-ΔC in the brain modulates the integrity of neurons, and may be involved in the pathogenesis of the neuronal abnormalities observed in the late stages of the disease.

Conclusions: We identified the presence of CRMP-2-ΔC in the brain of a murine model of prion disease. Of note, C-terminal truncations of CRMP-2 have been recently observed in models for neurodegenerative disorders such as ischemia, traumatic brain injury, and Wallerian degeneration. While the structural identity of CRMP-2-ΔC in those models remains unknown, the present study should provide clues to the molecular pathology of degenerating neurons in prion diseases in connection with other neurodegenerative disorders.

Background

Transmissible spongiform encephalopathies, or prion diseases, are fatal neurodegenerative disorders that include Creutzfeldt-Jakob disease, Gerstmann-Sträussler-Scheinker disease, fatal familial insomnia and kuru in humans, scrapie in sheep and goats, and bovine spongiform encephalopathy in cattle. The diseases are characterized by the accumulation of the disease-associated form(s) of prion protein (PrP^{Sc}) in the central nervous system and neuronal loss and vacuolation, although these features are not evident in some cases [1]. Analyses in murine models of scrapie showed that the neuropathological changes begin with the local deposition of PrP^{Sc}, followed by axon terminal degeneration,

* Correspondence: hagiwark@nih.go.jp
[1]Department of Biochemistry and Cell Biology, National Institute of Infectious Diseases, 1-23-1, Toyama, Shinjuku-ku, Tokyo 162-8640, Japan
Full list of author information is available at the end of the article

synaptic loss, and atrophy of dendritic trees in the lesions [2,3]. PrP^{Sc} is a conformational isoform of the cellular prion protein (PrP^{C}) encoded by the host *prnp* gene. While PrP^{C} is susceptible to digestion by proteinase K (PK), PrP^{Sc} is partially resistant to PK and is considered to be the infectious agent [1,4].

PrP^{C} is a glycosylphosphatidylinositol-anchored protein, and resides in the so-called lipid raft domains of the outer leaflets of plasma membranes, in endosomes, and in lysosomes [1]. An electron microscopic analysis showed the distribution of PrP^{C} on the plasma membranes of dendrites and spines, as well as in dendritic transport vesicles, endosomes, the axolemma, axonal transport vesicles and the myelin sheath [5]. Its physiological functions remain unknown, but it is proposed to be involved in cell-to-cell recognition, signal transduction by coupling with certain transmembrane-type receptors, response to oxidative stress, or the uptake of metal ions into cells [6]. Nevertheless, the observation that *prnp*$^{-/-}$ mice are viable [7] indicates the functional redundancy of PrP^{C}, and raises the question of whether a 'loss-of-function' of PrP^{C} is responsible for the neuronal cell death [8]. It is equally unclear whether PrP^{Sc} triggers neuronal cell death [8]. To understand the molecular neuropathology of prion diseases, microarray-based gene expression profiling has been conducted in murine models [9-13] and in cultured cells infected with the scrapie agent [14]. Proteomic analysis also identified 54 proteins differentially expressed in prion-infected cultured cells [15]. However, DNA microarray-based approaches [9-14] cannot detect the post-translational modifications of proteins, and the proteomic analysis in cultured cells [15] focused on the quantitative changes of proteins rather than their post-translational modifications.

In this study, we conducted a proteomic analysis of the brain in a murine model of scrapie to explore the molecular neuropathology of prion disease, and identified a truncated form of collapsin response mediator protein-2 (CRMP-2). Liquid chromatography-electrospray ionization-tandem mass spectrometry (LC-ESI-MS/MS) revealed that the truncation occurred on the carboxylic side of Ser^{517}. CRMP-2, also known as CRMP-62, dihydropyrimidinase-related protein 2, Unc-33-like protein, or TOAD-64 [16-19], is a mediator of axonal outgrowth and axon-dendrite specification [16-20], and its activity is regulated through the sequential phosphorylation of its carboxyl-terminal (C-terminal) region by Cdk5 and GSK-3β or by Rho-kinase [20]. As the truncation at Ser^{517} caused the partial ablation of the C-terminal phosphorylation sites, we further examined if the truncation affects the morphology of neurites in primary cultured neuronal cells.

Results

Two-dimensional electrophoresis of the soluble fractions from brain homogenates

Female C57BL/6J and ICR mice inoculated intracerebrally with prion (Obihiro-I strain) [21] began to show symptoms at approximately 130 days after inoculation (dai), fell ill by 170 dai, and were euthanized by 190 dai having entered the terminal stage. The accumulation of PrP^{Sc} in the brain became detectable by Western blotting at approximately 100 dai and was obvious from 130 dai (see below), as previously reported [22]. By contrast, the mock-infected control mice were healthy throughout the experiment. Using two-dimensional electrophoresis (2-DE) analysis and matrix-assisted laser desorption/ionization-mass spectrometry (MALDI-MS) (C57BL/6J sacrificed at 40, 69, 101, 133, and 160 dai, n = 2; ICR at 32, 70, 116, and 152 dai, n = 3), we found increases in the levels of glutathione S-transferase-μ1 and peroxiredoxin-6 (Figures 1A, B, and 1C, spots 4 and 5, respectively; Table 1). We also detected an increased abundance of glial fibrillary acidic protein (GFAP) in the infected mice (Figure 1B, spots 1-3; Table 1), as previously reported [9-11,13,23,24].

During the analysis, we were particularly interested in spots *a*, *b1*, *b2*, and *b3*, named according to their *acidic* or *basic* pI values (Figure 1). The intensity of spot *a* increased with the progression of the disease in ICR mice (Figure 1B) and C57BL/6J mice (not shown), whereas the intensity of spots *b1*, *b2*, and *b3* decreased (Figure 1B). We also found that the intensity corresponding to spot *a* remained very weak in the mock control mice (Figure 1D). MS analysis demonstrated that spots *a*, *b1*, *b2*, and *b3* invariably contained CRMP-2 (Table 1). This result was further confirmed by Western blot analysis with an anti-CRMP-2 antibody (C4G) (Figure 1E). The antibody revealed several additional spots undetectable by SYPRO Ruby staining due to their low abundance (compare Figures 1D and 1E). These spots appeared to reflect the diverse levels of phosphorylation because each spot was separated by an almost constant pI value that was indicative of protein phosphorylation [25,26], and because treatment with λ-phosphatase (λ-PPase) [27] prior to the 2-DE/Western blot analysis eliminated the spots in the acidic region (Figure 1E, top and bottom). Spot *b1* had an observed molecular mass (Mr_{obs}) of 61 kDa and pI (pI_{obs}) of 5.77 (Table 1) that were close to the theoretical Mr (62,278 Da) and pI (5.95) of the non-phosphorylated full-length CRMP-2. On the other hand, spot *a* had an Mr_{obs} of approximately 56 kDa and a pI_{obs} of 5.45 (Table 1), and the λ-PPase treatment did not affect its electrophoretic mobility (compare Figure 1E, top and bottom).

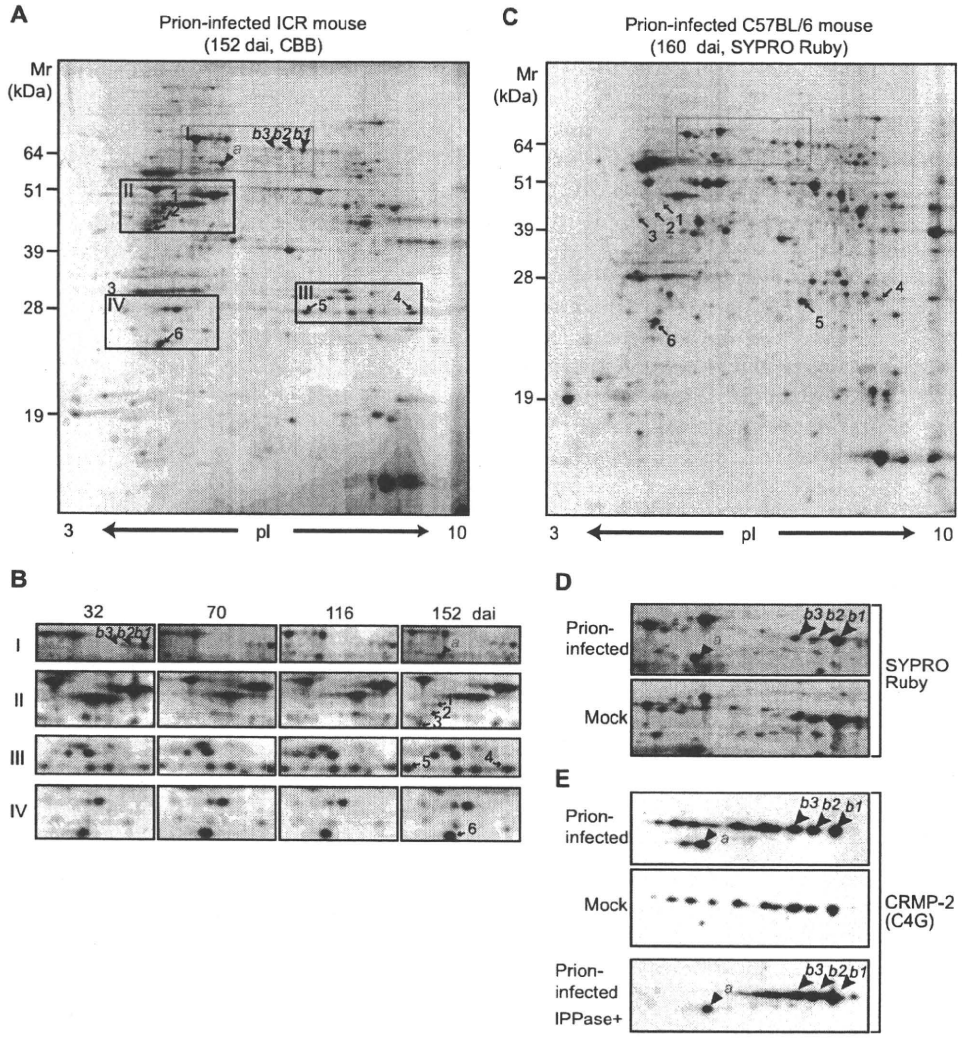

Figure 1 Two-DE analysis of soluble brain fractions. (A and B) CBB-stained gel obtained from a prion-infected ICR mouse (152 dai), and magnified images of boxes I-IV. The numbered spots differed in signal intensity between the prion-infected mice and the mock-infected controls, and were identified as listed in Table 1. (C) SYPRO Ruby-stained gel obtained from a prion-infected C57BL/6J mouse (160 dai). (D) The magnified image of the boxed area in (C) in comparison with the corresponding area of a 2-DE gel from a control C57BL/6J mouse. (E) Western blot analysis using the C4G anti-CRMP-2 antibody on the corresponding samples in (D). The lower panel shows the sample pre-incubated with λ-PPase.

Structural elucidation of the 56-kDa form of CRMP-2 by LC-ESI-MS/MS

To elucidate the structure of CRMP-2 in spots *a* (56 kDa) and *b1* (61 kDa), we compared the tryptic peptides derived from the two spots by LC-ESI-MS/MS (Figure 2). In addition to the peptides detected in both digests (Figure 3, shown in grey), spot *b1* yielded C-terminal peptides (Figure 3, indicated by boxes) including Ile^{558}-Arg^{565} ($[M+H]^+$ = 766.5), Glu^{526}-Arg^{532} ($[M+H]^+$ = 778.5) (Figure 2A, an asterisk at 13.2 min), and Ala^{566}-Gly^{572} ($[M+H]^+$ = 675.3) (Figure 2A, an asterisk at 17.5 min). Recovery of these C-terminal peptides, together with the Mr_{obs} (61 kDa), indicated that CRMP-2 in spot *b1* was the full-length form. Conversely, the digest derived from spot *a* did not yield these C-terminal peptides (Figure 3). We then digested CRMP-2 in spots *a* and *b1* using endoproteinase Glu-C (Glu-C) (Figure 2B). Full-length form of CRMP-2 is expected to release the C-terminal fragment Val^{506}-Asp^{547} (broken line in Figure 3) on digestion with Glu-C. However, this peptide

Table 1 Summary of the mass spectrometry analysis

	2-DE[b]		Mass spectrometry						Theoretical[b]		Fold change[d] (160dai)	p[e]
Spot[a]	Mr_{obs} (kDa)	pI_{obs}	Method	Identity	UniProt KB accession	Coverage	Number of peptides	Mowse score[c]	Mr_{cal} (kDa)	pI_{cal}		
a	56	5.45	MALDI & LC-ESI	CRMP-2-ΔC	O08553	39	17	963	56.5[f]	5.48[f]	7.96	0.076
b1	61	5.77	MALDI & LC-ESI	CRMP-2	O08553	45	22	1419	62.3[g]	5.95[g]	0.53	0.375
b2	61	5.72	MALDI & LC-ESI	CRMP-2	O08553	8	4	61	62.3	5.95[h]	0.39	0.249
b3	61	5.68	MALDI & LC-ESI	CRMP-2	O08553	7	4	103	62.3	5.95[h]	0.51	0.350
1	43	5.1	MALDI	GFAP	P03995	39	13	79	49.9	5.28	0.85	0.823
2	41	5.02	MALDI	GFAP	P03995	48	18	155	49.9	5.28	1.33	0.628
3	40	4.85	MALDI	GFAP	P03995	25	9	66	49.9	5.28	8.93	0.056
4	27	7.4	LC-ESI	Glutathione S-transferase μ1	P10649	21	7	176	25.8	8.14	+++[i]	ND
5	26	5.79	MALDI	Peroxiredoxin -6	O08709	44	8	121	24.7	5.72	1.58	0.389
6	24	5.02	LC-ESI	Peroxiredoxin -2	Q61171	38	8	372	21.6	5.2	0.90	0.850

a) The spots shown in Figure 1.

b) Mr_{obs} and Mr_{cal}, observed and theoretical Mr; pI_{obs} and pI_{cal}, observed and theoretical pI, respectively.

c) Probability-based Mowse score [52] calculated using MASCOT software [48].

d) Fold change of spot volume on 160 dai.

e) *p*-Value of Student's t-test. ND: not determined.

f) Mr_{cal} and pI_{cal} of non-phosphorylated CRMP-$2^{1\text{-}517}$.

g) Mr_{cal} and pI_{cal} of non-phosphorylated CRMP-$2^{1\text{-}572}$.

h) An approximate shift of -0.05 per phosphate moiety is expected [25,26].

i) Undetectable in the mock sample.

was not detected in the digest of spot *a*; instead, the digest of spot *a* but not spot *b* gave rise to a unique peak in the chromatogram (an asterisk at 25.2 min in Figure 2B). MS analysis of this peak fraction detected three ion peaks at *m/z* values of 594.4, 913.7, and 1186.8 (Figure 2B). Subsequent LC-ESI-MS/MS analysis determined that the ion peaks at *m/z* 1186.8 ($[M+H]^+$) and 594.4 ($[M+2H]^{2+}$) were derived from the peptide Val^{506}-Ser^{517} (Figure 2D), while the ion peak at *m/z* = 913.7 ($[M+H]^+$) was ascribed to a b-type ion of Val^{506}-Thr^{514} (Figure 2C). This b-type ion may be produced by the fragmentation of the parental peptide Val^{506}Ser-ValThrProLysThrValThr^{514}Pro^{515}AlaSer^{517} between the Thr^{514}-Pro^{515} bond, such a fragmentation between -X^n–Pro^{n+1}- to release b_n and y_{N-n} ions (Gly and Pro are unfavorable for X, *N* is the total number of amino acids) being observed in tandem MS [28]. Because Glu-C hydrolyzes Glu-X and Asp-X bonds, the presence of a Ser residue at the C-terminus strongly suggested that the peptides were originally at the C-terminus of CRMP-2 in spot *a*. In support of this, the values of Mr_{obs} and pI_{obs} of spot *a* were in good accord with the corresponding theoretical values for non-phosphorylated CRMP-$2^{1\text{-}517}$ (Table 1). Therefore, we concluded that the 56-kDa CRMP-2 in spot *a* was truncated at Ser^{517}, and designated this shortened form CRMP-2-ΔC.

The ratio of CRMP-2-ΔC to full-length CRMP-2 during the progression of prion disease

Completion of the structural analysis of CRMP-2-ΔC enabled us to use the N3E antibody to evaluate the relative amounts of CRMP-2-ΔC (56 κDa) and the full-length form (61 κDa). Since the full-length CRMP-2 and CRMP-2-ΔC both contain the epitope for the N3E antibody which recognizes the amino acid sequence 142-194 of CRMP-2 [29], the antibody should give comparable signal intensities of the two forms in Western blot analysis. We observed that the ratio of the amount of CRMP-2-ΔC (56 kDa) to the total amount of CRMP-2 (56 kDa + 61 kDa) was negligible at 40, 69, and 101 dai, and increased slightly at 133 dai in the prion-infected mice and the mock-infected controls (Figures 4A and 4B). In the controls sacrificed at 160 dai, the ratio increased in a narrow range and did not exceed 0.3 (Figure 4B, right). By contrast, in the prion-infected mice sacrificed at 160 dai when the expression of GFAP was up-regulated (Figure 4A), CRMP-2-ΔC increased moderately whereas the full-length form decreased. As a

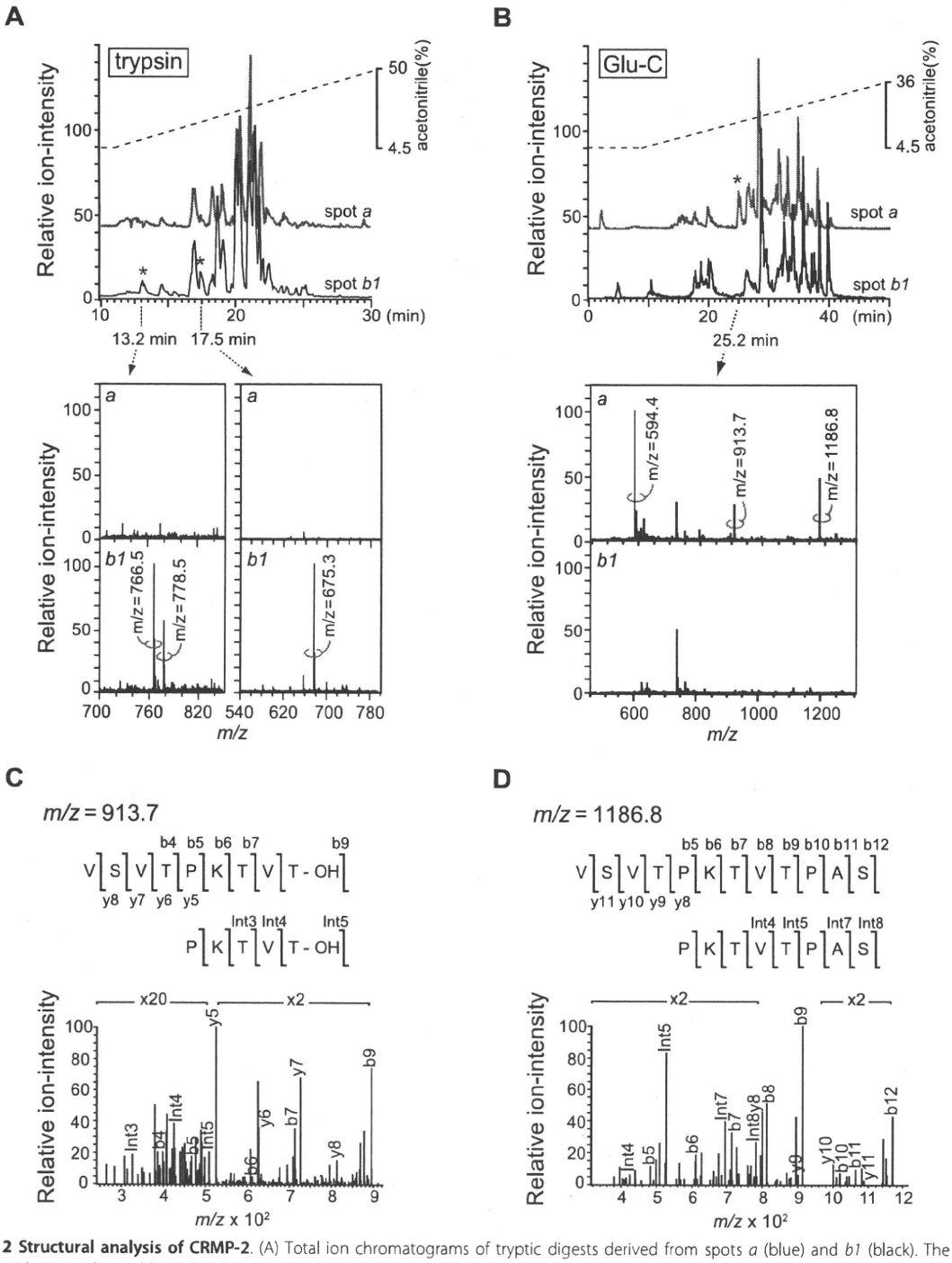

Figure 2 Structural analysis of CRMP-2. (A) Total ion chromatograms of tryptic digests derived from spots *a* (blue) and *b1* (black). The peaks with asterisks were detectable in the digest of spot *b1*, but not spot *a*. Lower panels show the MS spectra of the fractions eluted at 13.2 min and 17.5 min, and the amino acid sequences determined by LC-ESI-MS/MS. (B) Total ion chromatograms from the Glu-C digest of spots *a* (blue) and *b1* (black). The peak with an asterisk was detectable in the digests of spot *a*, but not spot *b1*. Lower panels show the MS spectra of the fraction eluted at 25.2 min, and the determined amino acid sequences. (C) LC-ESI-MS/MS spectrum and the sequence of the parental ion of m/z = 913.7. This parental ion was the b9 ion with a loss of a hydroxyl (-OH) group. The gain of the detector was modulated as indicated (× 2 or × 20 amplification) to optimize data acquisition. (D) MS/MS spectrum and the sequence of the parental ion of m/z = 1186.8.